*Citation for published version:*
Papatzani, S, Badogiannis, E & Paine, K 2018, 'The pozzolanic properties of inorganic and organomodified nano-montmorillonite dispersions', Construction and Building Materials, vol. 167, pp. 299-316. https://doi.org/10.1016/j.conbuildmat.2018.01.123

*DOI:*
10.1016/j.conbuildmat.2018.01.123

*Publication date:*
2018

*Document Version*
Peer reviewed version

Link to publication

*Publisher Rights*
CC BY-NC-ND

**University of Bath**

**General rights**
Copyright and moral rights for the publications made accessible in the public portal are retained by the authors and/or other copyright owners and it is a condition of accessing publications that users recognise and abide by the legal requirements associated with these rights.

**Take down policy**
If you believe that this document breaches copyright please contact us providing details, and we will remove access to the work immediately and investigate your claim.

Download date: 22. May. 2019

# The pozzolanic properties of inorganic and organomodified nano-montmorillonite dispersions

Styliani Papatzani[1,2,*], Efstratios G. Badogiannis[3] and Kevin Paine[1]

[1]*BRE Centre for Innovative Construction Materials, University of Bath, BA2 7AY, Bath, UK*

[2] *Greek Ministry of Culture, Directorate of Restoration of Medieval and Post-medieval Monuments, Tzireon 8-10, 11742, Athens, Greece, Country*

[3] *Civil Engineering Department, National Technical University of Athens, Athens 15773, Greece*

*Corresponding author: E-mail: spapatzani@gmail.com, Tel +30 6985877730

Abstract

The pozzolanic potentials of three non-thermally treated, nano-montmorillonite (NMt) dispersions were investigated by a new method involving the analysis of NMt/lime putty pastes via TGA/dTG and XRD crystallographic and semi-quantitative analysis. The criterion conceived was validated at eight days and eight months and was additionally verified via the Chapelle method. The inorganic NMt dispersion showed the most pronounced pozzolanic behaviour promoting $Ca(OH)_2$ consumption towards calcium

silicate/aluminate hydrates formation and binding behaviour. The two organomodified NMt dispersions exhibited pozzolanicity increasing with time. The results can pave the way for advances in cement science and restoration mortars development for historical structures rehabilitation, where low $CO_2$-footprint, natural inorganic materials are a prerequisite.

Keywords: inorganic and organomodified nano-montmorillonite dispersions, lime putty pastes, XRD, TGA/dTG, pozzolanic reactions, Chapelle test, non-calcined

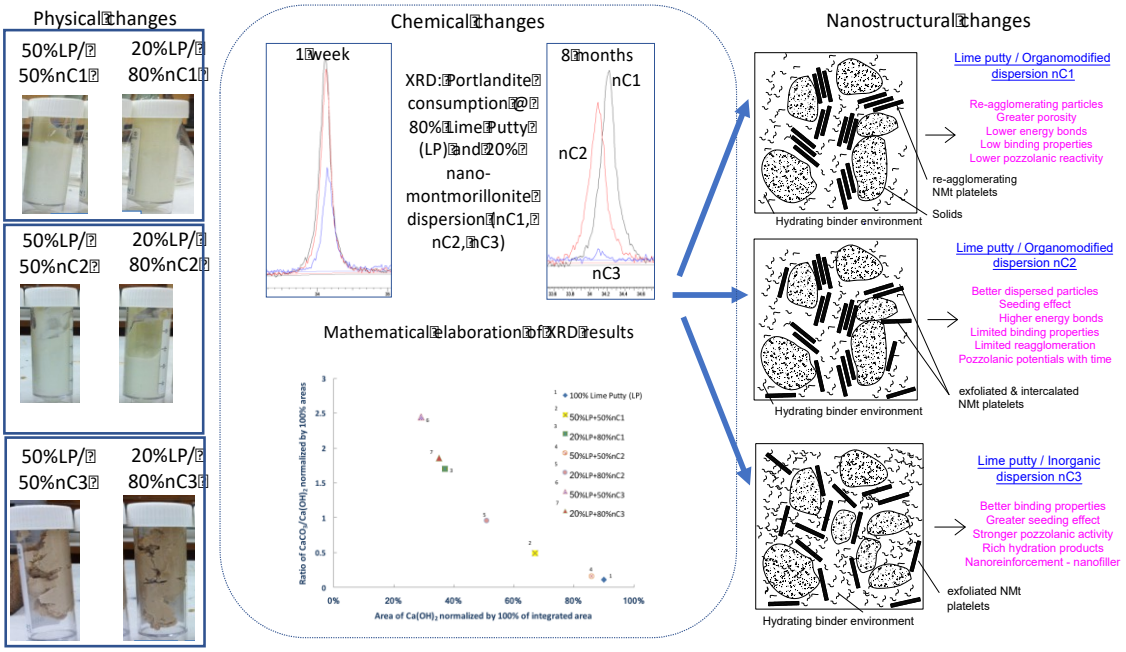


Graphical Abstract

## 1. Introduction

Montmorillonite (Mt) is one of the main minerals found in bentonites, a naturally occurring clay. Mt is rich in stacks of layers/platelets held together by interlayer cations, by van der Waals forces, by electrostatic force or by hydrogen bonding inhibiting the solubility or miscibility [1]. Moreover, Mt is a 2:1 layered silicate, implying that each layer is composed of two silicon tetrahedral sheets bonding with one octahedral sheet of alumina between them. Isomorphous substitution takes place in the octahedral sheet where most hydroxyl groups are located apart from the broken sides of each particle [2]. Surface modifiers, such as quaternary ammonium salts (quats) inserted in the interlayer space can fully separate these platelets (exfoliation or if at a lower extent, intercalation), creating individual nano-thick, plate-like particles. These particles, hereafter referred to as nano-montmorillonite (NMt), can engage in chemical reactions analogous to their specific surface area.

Apart from these organic modifiers, which usually cause platelet separation by cation exchange, and produce a pulverized product, Mt can be exfoliated in water in its pristine condition. In fact, even in earlier research focused on polymer-clay nanocomposites it has been stated that apart from organomodification, small additions of water were adequate for clay exfoliation [3]. Therefore, if Mt is dispersed in water, it can maintain its inorganic nature and platelets can remain dispersed with the help of inorganic surfactants. Inorganic surfactants promote the homogenous dispersion of the NMt platelets in the aqueous environment. NMt platelets dispersed in water are easier to handle compared to those in powder form, because agglomeration of particles into clusters (usually of micron scale or bigger) is avoided. In addition, NMt dispersed in water, provides greater miscibility with other cementing constituents.

55 The nanoengineering process of Mt layer separation and the NMt products have attracted the
56 attention of cement scientists who seek to use the exfoliated NMt particles as a means of
57 additional nucleation sites or nano-scale reinforcement in the hydrating cement matrix [4]. The
58 nature, nanostructure, production methods, effect of modifiers and dispersants and the
59 configurations of the NMt platelet separation for use as polymer nanocomposites or adsorption
60 materials can be found in the literature [3,5–7]. However, limited research is presented on the
61 use of NMt and this research is applied in cement binder formulations [4,8–10].

62 Supplementary cementitious materials (SCM) used in lime or cement mortars can be classified
63 as (i) pozzolanic (ii) latent-hydraulic or (iii) fillers. Pozzolanic SCM are the most common. A
64 pozzolanic SCM consists of a material rich in amorphous alumina or silica that is non-reactive
65 with other compounds and water as is to form additional hydration products. However, in the
66 alkaline medium created by the dissolution of calcium hydroxide in water the silicate or
67 aluminosilicate networks break down to form calcium silicate and/or calcium aluminate
68 hydrates. The relative pozzolanicity of a material depends on a high content of amorphous
69 phases and a high specific surface area.

70 With respect to pozzolanic studies on clays, at present only the pozzolanic activity of thermally
71 and mechanically treated kaolin [2,11,12] or halloysite nanoclay particles [13] has been
72 confirmed. There is disagreement on the pozzolanic potential of Mt with some researchers
73 stating that calcined Mt mineral exhibits limited pozzolanic activity depending on the
74 calcination temperature [2], while others claim that natural and calcined Mt contribute to
75 pozzolanic reactions [14]. That is to say, Mt so far has only been investigated in its calcined
76 form. However, the high temperatures involved for calcinations increase the $CO_2$ footprint of
77 the material. With the evolution of nanotechnology, which allows us to manipulate matter at
78 levels slightly above the atomic, another option rather than calcination arises; the

79 nanomodification of Mt, i.e. the breaking of the forces holding its platelets together so that the
80 nanoplatelets will then be individually available for reactions, as explained above. With respect
81 to NMt, the incorporation of Cloisite®30B to waste glass powder cement mortars exhibited
82 enhanced pozzolanic reactivity leading to improved mechanical properties [15]. In another
83 study the incorporation of Cloisite®30B to ordinary Portland cement showed pozzolanic
84 potentials [16]. Still, one element of the process is to nanomodify the Mt and another part is to
85 disperse it in water, so as to render it more compatible with binders, more easily usable with
86 higher potentials for mass production. So far, only the authors' team has presented research on
87 the effect of various NMt dispersions in the hydrating cement paste [4,8–10] and of this work
88 only part of it has proven the pozzolanic potentials of the inorganic NMt dispersion in ternary
89 Portland cement-limestone binders [8]. Therefore, although the pozzolanic contribution of NMt
90 in cement binders has been confirmed, the pozzolanic behaviour of NMt as a raw material is
91 yet to be scrutinized. However, given the complex nature of NMt dispersions, containing not
92 only Mt but also modifiers and dispersing agents, a criterion taking into account the
93 decomposition of various components within the same temperature intervals is yet to be
94 presented. This elaborate research will provide sound calculations of pozzolanicity in more
95 intricate matrices such as those of NMt enhanced cement binders.

96 The currently widely used pozzolanic additions such as fly ash, are being depleted [17] and
97 others such as silica fume are difficult to handle and increase the total cost of the binder. The
98 abundance of bentonite in nature, from which Mt can be received, and the ease of Mt
99 exfoliation in water in the case of inorganic dispersions [9,10], make NMt a potentially
100 interesting alternative SCM. Furthermore, the reaction of the exfoliated platelets around
101 hydrated Portland cement particles can enable a tortuous microcrack propagation pattern, hence
102 providing nanoreinforcement at the nanolevel to the microlevel, as confirmed by a series of

experiments [10]. Other clays, such as metakaolin, get activated by heating above 700°C, increasing the embodied $CO_2$ of the binder. Therefore, avoiding calcination and nanomodifying Mt, comprises a way of producing sustainable low carbon additions for the future. Given that the filler effect of Mt is confirmed [2], what remains to be assessed is the pozzolanic effect of NMt dispersions, which are easier to handle than their powder counterparts, however exhibit an inherent difficulty because of the presence of the modifier and surfactant.

The depletion of natural and man-made pozzolanas and the need to lower the carbon dioxide footprint by avoiding pozzolanas produced by calcination, is calling for new materials and methods to be developed. From the above, it can be established that neither the pozzolanic activity of non-calcined NMt nor the pozzolanicity of non-calcined NMt dispersions has been examined previously. Such a discovery could be proven valuable for cement science, because it will allow the use of NMt dispersions, whose main constituent, montmorillonite, is abundant in nature and environmentally friendly, as SCM, avoiding the otherwise added environmental cost of calcination. Therefore, this research programme was designed to investigate the pozzolanic properties of two different aqueous organomodified NMt dispersions and one aqueous inorganic NMt dispersion. Characterization techniques for this standalone methodology of assessing the pozzolanic behaviour only necessitated: thermal gravimetry analysis and differential thermogravimetry (TGA/dTG), X-Ray diffraction (XRD) crystallography and Semi-quantitative analysis based on XRD at 8 days and 8 months.

The application of this knowledge is suited for the characterization of NMt as a potential pozzolanic SCM can open a new horizon for the understanding of the effect and further development of nanoclays and NMt in cementitious composites and lime binders. Lastly, this study can further be elaborated for the development of new binders for cultural heritage conservation, referred to in detail in the discussion.

# 1. Materials and Methods

## 1.1. Materials

A commercially available lime putty was mixed at various concentrations with three aqueous dispersions of NMt as described below:

### 1.1.1. Organomodified nano-montmorillonite dispersions (nC1 and nC2)

A purified bentonite suspension [3.9% Mt and 96.1% water, Cation Exchange Capacity (CEC) 105 meq/100 g], produced by Laviosa Chimica Mineraria S.p.A., was organomodified by exchange of basal metal cations with methylbenzyl di-hydrogenated tallow ammonium chloride (Noramonium MB2HT) at Lietuvos Energetikos Institutas [18] producing NMt powder, named as XDB. This organomodified powder contained approximately 43% Noramonium MB2HT bound to the Mt and comprised the base for two organomodified dispersions. This proportion was confirmed by characterization of the starting material via thermogravimetric analyses as shown in the results section.

NMt powder XDB, was dispersed in water to avoid agglomeration, which would bring the material back to the micron scale. The side effect of the organomodification for cement chemistry is the creation of a hydrophobic nanocomposite, incompatible with water, causing extensive flocculation of particles, when dispersed. Surfactant technology was employed to leverage this fact and in specific:

(1) 5% by mass (non-ionic) fatty alcohol and 1% by mass defoaming agent was used to create nC1 dispersion, and

(2) 5% by mass (anionic) alkyl aryl sulphonate was used to create nC2 dispersion.

The NMt loading achieved for both the aqueous dispersions was 15% XDB.

### 1.1.2. Inorganic nano-montmorillonite dispersion (nC3)

The inorganic NMt powder used for the NMt dispersion is commercially available under the name Dellite®HPS. It was derived from the purification of bentonite by Laviosa Chimica Mineraria S.p.A. Dellite®HPS, is by nature compatible with water. However, the introduction of inorganic dispersant was necessary to overcome the electrostatic interaction of particles for high clay loading in aqueous solutions. Sodium polyphosphate was used for the dispersion of the inorganic NMt, in water. The NMt loading achieved in the aqueous dispersion was 15% HPS solids by total mass.

### 1.1.3. Lime Putty (LP)

A commercially available lime putty (LP) conforming to class CL 90 according to BS EN 459-1 norm was used [19].

## 1.2. Methods

### 1.2.1. Background

It is acknowledged that a number of standardised pozzolanic reactivity tests are established such as the Chapelle method, Fratinni method and Strength Activity Index [20]. However, the

Chapelle method is primarily valid for calcined clays, because the consumption of calcium hydroxide is only related to the amorphous and vitreous phase of a material. To the best knowledge of the authors it has never been applied for the characterization of non-calcined NMt dispersions. Moreover, the Fratinni and Strength Activity Index method necessitate the use of cement, which is already a composite material. Therefore, for this work, an innovative method was introduced by which non-thermally treated NMt enhanced lime putty pastes were prepared, allowed to harden and examined via XRD, TGA/dTG and a semi-quantitative analysis based on XRD at an age of 8 days and 8 months. The pastes employed for the suggested method were preferred to the traditional ones for the following reasons; (i) lime putty constitutes a highly reactive binding materials in comparison to the dry powder CaO used for the Chapelle method. In addition to this, lime putty exhibits a higher specific surface area conferring not only greater reactivity but also better rheological properties particularly when aged [21,22] (ii) lime putty's composition is simple (chemically unbound water easily separated by drying at 100°C [23]) compared to the complex chemical composition of Portland cement clinker, which is necessary for the Fratinni method and the Strength Activity Index, (iii) binary compositions allow for straight forward conclusions and (iv) such studies broaden our current knowledge on materials' combination for historic lime mortar conservation. That said, the starting NMt powders (HPS and XDB) and two of the dispersions (nC2 and nC3) were tested with the Chapelle method for comparison and for validation of the newly introduced method.

### 1.2.2. Experimental Procedure

The new method

A reference sample of LP was prepared by vigorous whisking of the material with a pallet knife until it was homogenized. 20 g of the plain LP sample were sealed in a vial.

100 g of the reference LP was dried at 60°C for 24 hours and another 100 g was dried at 100°C, to detect any differences in $Ca(OH)_2$ or surface water content. The procedure described in [23] was followed and the relationship established between lime slaking time and amount of free water was confirmed, i.e. after 24 hours of drying immediately after slaking the amount of free water measured reached 60% by mass in accordance with BS EN 459-1 [19] and suggestion by Moropoulou et al [24] that free water content should not exceed 60% by mass.

Six NMt modified lime putty pastes were prepared as shown in

Table **1**. The mix proportions of NMt refer to the NMt dispersion rather than NMt solids only. Materials were manually mixed due to the small quantities required, with a spatula for 1 minute and the pastes were placed in vials. All vials were immediately sealed with their cap, protected with tape and further secured in a sealed, airtight bag to avoid contact with the $CO_2$ present in air and consequently carbonation, in order to only study the pozzolanic reaction.

The only moment when the samples were in contact with air (i.e. when carbonation could have taken place by the formation of calcium carbonate), was during mixing of the pastes or during crushing or testing. Because these moments were quite limited and carbonation is a self-limiting reaction, it can be assumed that the amount of $CaCO_3$ precipitated by carbonation is limited and can be disregarded for the 8-days-old pastes. If carbonation takes place then the hydrated

compounds (such as $Ca(OH)_2$ and calcium silicate hydrates (C–S–H) [25]) will also have been carbonated [26].

Samples were cured for two different periods: (i) 6 days at room temperature and consecutively oven-dried for 36 hours and tested at day 8 and (ii) 238 days at room temperature and consecutively oven-dried for 36 hours and tested at 8 months (240 days). Only the LP/nC3 pastes set immediately, whereas the remaining four formulations were still unhardened after the six-day period, as can be seen in Figure 1; the fact that nC3 exhibited a more pronounced binding activity could possibly be attributed to greater pozzolanicity (sample number 3 and 6 in Figure 1 and Table 1).

Table 1: Composition of LP/nC1, LP /nC2, LP/nC3 pastes

| **Sample** | **Sample No in Figure 1** | **LP content (% mass)** | **Dispersion content (% mass)** |
|---|---|---|---|
| 100% LP | | 100 | 0 |
| 50% LP + 50% nC1 dispersion | 1 | 50 | 50 |
| 50% LP + 50% nC2 dispersion | 2 | 50 | 50 |
| 50% LP + 50% nC3 dispersion | 3 | 50 | 50 |
| 20% LP + 80% nC1 dispersion | 4 | 20 | 80 |
| 20% LP + 80% nC2 dispersion | 5 | 20 | 80 |
| 20% LP + 80% nC3 dispersion | 6 | 20 | 80 |

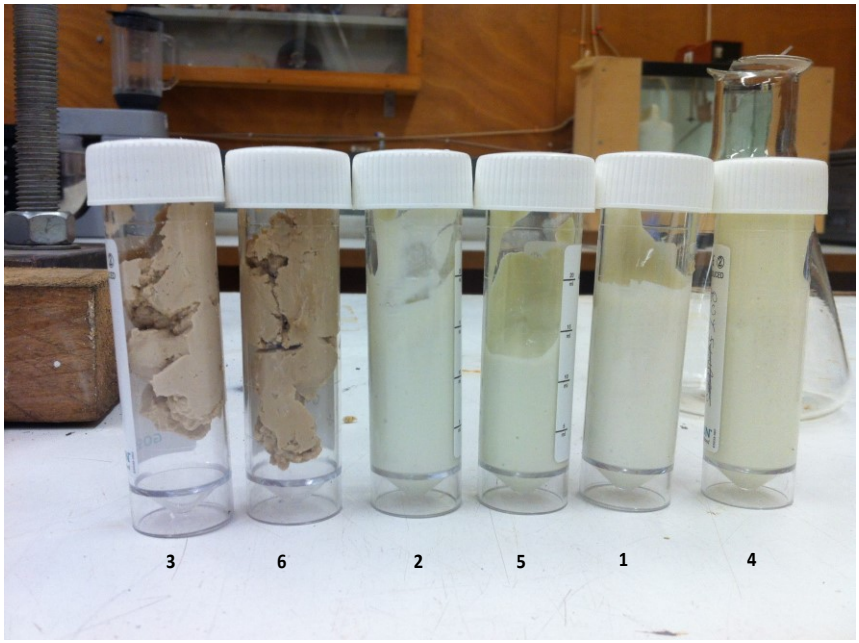


228

229 Figure 1: Characteristics of LP/nC1, LP /nC2, LP/nC3 pastes after six days of curing and
230 before oven-drying

231

232 When the six-day period had passed, the pastes were oven-dried at 60°C for 24 hours. After
233 oven drying was complete, the samples were crushed to powder passing through a 125 μm
234 sieve. It should be noted that the LP/nC2 as well as the LP/nC1 were extremely soft and fine
235 upon grinding. On the contrary, the LP/nC3 pastes were very hard to break and to grind. Ground
236 powdered samples were poured in vials and were allowed to dry for a further 12h in a desiccator
237 (to avoid carbonation or sample contamination) placed in the oven at 60°C.

238 The procedure was repeated 8 months later for the study of the ageing process of the same
239 pastes.

240

Validation of the new method via the Chapelle test

The pozzolanic activity of the starting NMt powders [XDB (discussed in section 1.1.1) and Dellite®HPS (abbreviated as HPS and discussed in section 1.1.2)] and two of the dispersions (nC2 and nC3) were confirmed by the Chapelle test [27,28]; 1g of each sample was mixed with 1 g of $Ca(OH)_2$ and 100 ml of boiled water. The suspension was boiled for 16 h and the free $Ca(OH)_2$ was determined by means of sucrose extraction and titration with a HCl solution. Powders of the Chapelle products were tested via X-ray diffraction and compared with raw NMt powders and dispersions.

### 1.2.3 Analytical techniques

Mineralogy was investigated via XRD and the thermal properties via TGA/dTG. The consumption of calcium hydroxide was further evaluated with the adoption of a semi-quantitative method.

#### X-ray diffraction (XRD)

XRD measurements were performed using a D8 ADVANCE x-ray diffractometer with $CuK_\alpha$ radiation. Spectra were obtained in the range $4^o < 2\theta < 60^o$ at an angular step-size of 0.016° $2\theta$. Analysis of reflections and d-value were calculated according to Bragg's law ($n\lambda = 2d\sin\theta$) [29]. WiRE™ software [30] was used for mathematical curve fitting (polynomial smoothing) of the XRD diffractograms, and EVA software [31] was used to determine the mineralogy and

integrated area. The most matching compounds formed were selected based on the elemental analysis of the nano-montmorillonite dispersions [10].

**Thermal gravimetric analyses (TGA)**

Thermal gravimetric analyses (TGA) were carried out using a Setaram TGA92 instrument. 20 mg of each sample were placed in an alumina crucible and heated at a rate of 10°C/min from 20°C to 1000°C under 100 mL/min flow of inert nitrogen gas. The differential thermal gravimetric (TGA/dTG) curve was derived from the TG curve. Buoyancy effects were taken into account, by correcting the curves via automatic blank curve subtraction. TG analyses were carried out on oven-dried samples instead of wet ones. This was to differentiate, at 100-140°C, between the mass loss that may be attributed to the decomposition of calcium silicate hydrate, from the mass loss that may be attributed to water evaporation from the pores of the samples. Moreover, greater convergence with XRD results can be expected if samples are in the same state. Therefore, since XRD analysis must be carried out in powders, the same state was preferred for TGA.

**1.2.4. Mathematical elaboration**

Decomposition stages of LP/nC1, LP/nC2 and LP/nC3 pastes

In order for the method to yield results, the net amount of $Ca(OH)_2$ consumed must be calculated. That is to say, the amount of NMt decomposing within the specific temperature range as that for $Ca(OH)_2$ i.e. *400-500°C,* must be subtracted from the total mass loss recorded by applying the following formulae:

$M_{CH} = M_{loss}^{400\text{-}500} - M_{NMt}^{400\text{-}500}$ x (%NMt) Equation: 1

Where,

$M_{CH}$ = *Mass loss related to* $Ca(OH)_2$

$M_{loss}^{400\text{-}500}$ = Mass loss of LP/NMt paste recorded by TG between 400-500ºC

$M_{NMt}^{400\text{-}500}$ = Mass loss of dried NMt recorded by TG between 400-500ºC

(%NMt) = [% of NMt dispersion present in the paste (i.e. 50% or 80%)]

It is assumed that the mass loss of dried NMt recorded by TG between 400-500ºC is proportional to its original percentage in the mix.

Accordingly, the net mass loss related to $CaCO_3$ must be calculated by subtracting from the total mass loss the amount of NMt decomposing within the specific temperature range, i.e. 600-800ºC, according to the following formulae:

$M_{CC} = M_{loss}^{600\text{-}800} - M_{NMt}^{600\text{-}800}$ x (%NMt) Equation: 2

Where,

$M_{CC}$ = Mass loss related to $CaCO_3$

$M_{loss}^{600\text{-}800}$ = Mass loss of LP/NMt paste recorded by TG between 600-800ºC

$M_{NMt}^{600\text{-}800}$ = *Mass loss of dried* NMt *recorded by TG between 600-800ºC*

(%NMt) = *[% of* NMt dispersion *present in the paste (i.e. 50% or 80%)]*

As assumed above, the mass loss of dried NMt recorded by TG between 600-800ºC is proportional to its original percentage in the mix.

Mass calculations

For the area associated with the dehydration of $Ca(OH)_2$ between 400ºC and 510ºC the following chemical reaction applies:

$$Ca(OH)_2 \rightarrow CaO + H_2O \uparrow$$

The amount of $Ca(OH)_2$ present in the paste at different ages can be computed by the stoichiometric elaboration of the mass loss results within the specific temperature range:

$$MM_{CH} = \frac{M_{CH} \times 74.0930}{18.0153} \Longrightarrow MM_{CH} = \frac{M_{CH}}{0.243} \quad \text{Equation: 3}$$

Where,

$MM_{CH}$ = mass of $Ca(OH)_2$

$M_{CH}$ = *Mass loss related to* $Ca(OH)_2$ measured by TGA

18.0153 g/mol = molecular mass of $H_2O$ and 74.0930 g/mol = molecular mass of $Ca(OH)_2$.

Similarly, the decomposition of $CaCO_3$ occurs between 700ºC and 810ºC according to the following chemical reaction [32]:

$$CaCO_3 \rightarrow CaO + CO_2 \uparrow$$

The amount of $CaCO_3$ present in the paste at different ages can be computed by the stoichiometric elaboration of the mass loss results within the specific temperature range:

$$MM_{CC} = \frac{M_{CC} \times 100.0869}{44.0100} \Longrightarrow MM_{CC} = \frac{M_{CC}}{0.44} \quad \text{Equation: 4}$$

Where,

$MM_{CC}$ = mass *of* $CaCO_3$

322 $M_{CC}$ = *Mass loss related to* $CaCO_3$ measured by TGA

323 100.0869 g/mol = molecular mass of $CaCO_3$ and 44.0100 g/mol = molecular mass of $CO_2$

324

325 Carbonation recalculations

326 Furthermore, the reference LP paste and all LP/NMt pastes had carbonated. As a result, the total
327 molar mass related to $Ca(OH)_2$ had to be recalculated:

328

329 By assuming that all of this calcium carbonate (mass loss traced above $600^oC$) was once
330 calcium hydroxide:

331 $Ca(OH)_2 + CO_2 \rightarrow CaCO_3 + H_2O$

332 Which in molar mass terms is: 74.0930 + 44.0100 → 100.0869 + 18.0153, therefore:

333 Mass of $Ca(OH)_2$ that has carbonated = $MM_{carbCH}$ = [$MM_{CC}$] / [(100.0869 /74.0930)] = $MM_{CC}$ /
334 1.35

335 Therefore:

336 $MM_{totCH} = MM_{CH} + MM_{carbCH}$ Equation: 5

337 Where,

338 $MM_{totCH}$ = Total mass of $Ca(OH)_2$ prior to carbonation

339 $MM_{CH}$ = Mass of $Ca(OH)_2$ as calculated by Equation 3

340 $MM_{carbCH}$ = $MM_{CC}$ / 1.35 = Mass of $Ca(OH)_2$ that has carbonated (i.e. mass loss traced above
341 600°C as calculated by Equation 2 and 4)

342 # 2. Results and Discussion

343 ## 2.1. X-ray Diffraction (XRD)

344 The consumption of $Ca(OH)_2$ (Portlandite or CH) by the three different NMt dispersions was at
345 first confirmed by XRD analyses carried out at both 8-day and 8-month old powders (Figure 2).
346 In terms of mineral and phase identification, Montmorillonite particles with
347 different sizes, have been differentiated according to previous work carried out by the authors
348 [10]. Graphs A and B identify a pick as being Mt. Diffractograms show that reflections assigned
349 to Portlandite reduce with time. Moreover, the higher the nC1, nC2 or nC3 content the greater
350 the Portlandite consumption. This reduction was more pronounced for nC3. In fact, in
351 agreement with the TG analysis which follows, Portlandite almost disappeared for the
352 20%LP80%nC3 paste at day 8, whereas for month 8 it was completely eliminated. Interestingly,
353 nC3 showed high crystallization with montmorillonite and Portlandite reflections transforming
354 into sodalite, calcium silicate and caresite for the 50%LP50%nC3 paste at 8 months and
355 significant quantities of calcium aluminum oxide carbonate hydrate, a major cementing
356 compound [33] for the 20%LP80%nC3 paste at month 8.

357 Dispersions nC1 and nC2 exhibited similar $Ca(OH)_2$ consumption, with nC1 being slightly
358 more reactive towards the production of calcium-containing hydrate compounds. In fact, the C–
359 S–H is amorphous and its presence may be recorded by humps appearing between 20 and 30°2$\theta$
360 [2,34]. All XRD spectra of the LP/NMt pastes present such a hump approximately at 20°2$\theta$, that

is to say, after the Portlandite peak at 18.2°2$\theta$. In fact, for all nC2 enhanced pastes only the C–S–H humps were identified and no crystal compounds were detected.

Furthermore, of strätlingite [$Ca_2Al((AlSi)_{1.11}O_2)(OH)_{12}(H_2O)_{2.25}$] were traced for the 50%LP50%nC1 paste at 8 days and quantities of C–S–H were identified for the 20%LP80%nC1 paste at day 8. At this point it should be noted there has been a debate on the nature of the C–S–H structure and it has recently been postulated, that although amorphous, at the nanolevel it exhibits a highly ordered structure [25]. Therefore, it is possible that even by XRD analyses, diffractions recorded as humps can assist towards the validations of such findings. After 8 months, it seems that montmorillonite was transformed into Stichtite [$Mg_6Cr_2CO_3(OH)_{16}$ 4 $H_2O$] for both 50%LP50%nC1 and 20%LP80%nC1 pastes.

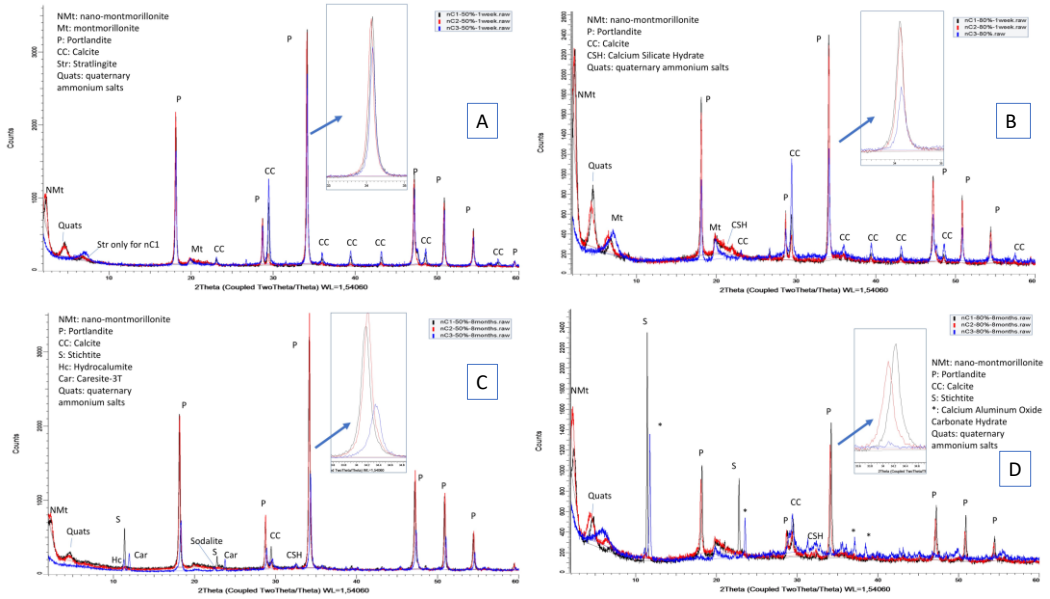


Figure 2: XRD analyses of (A) 50%LP+50%nC1/nC2/nC3 dispersions - at day 8, (B): 20%LP+80%nC1/nC2/nC3 dispersions - at day 8, (C) 50%LP+50%nC1/nC2/nC3 dispersions - at month 8 and (D) 20%LP+80%nC1/nC2/nC3 dispersions - at month 8

## 2.2. Semi-quantitative analysis based on XRD

A semi-quantitative analysis was developed on the grounds of comparison of the integrated areas (wide rectangle in Figure 3) under the two adjacent reflections of $Ca(OH)_2$ at 28.7º2$\theta$ and $CaCO_3$ at 29.4º2$\theta$. Polynomial curve fitting was performed to smoothen the XRD results and even out minor noise (as seen in Figure 3). The calcite traced in the nC3 enhanced pastes just below 30º2$\theta$ angle, is attributed to the Mg-calcite naturally present in Mt, whereas the calcite identified in nC1 enhanced pastes can be related to the high quantities of organic matter traced in the characterization of the starting nano-montmorillonite powders [9]. For the 8-month-old pastes the presence of $CO_3$ containing compounds is typical of carbonation process [33]. The reduction of the Portlandite peak can only be compared between the same LP content pastes and no comparisons should be made between the 50% and 80% nC content pastes because the starting Portlandite (CH) is different. Therefore, for day 8, none of the 50%LP pastes showed significant reduction, whereas for the 20%LP pastes, nC3 dispersion showed the highest consumption (lowest relative peak intensity in Figure 3). Similarly, for month 8, nC3, followed by nC1, showed the highest CH consumption for the 50%LP pastes, whereas for the 20%LP pastes, CH was extinct in the nC3 enhanced pastes.

Next, EVA software [31] was used for the determination of the areas under the 28.7º2$\theta$ and 29.4º2$\theta$ angles' peak. The integrated area comprises the total area under both adjacent reflections. The results of these analyses are depicted in Figure 4, with the consumption of $Ca(OH)_2$ clearly identified particularly by nC3 enhanced pastes in both ages. It can be, hence, concluded that XRD can give an estimation on the quantities of CH and calcium carbonate present in the bulk powder sample, however a more elaborate procedure is still required in order to differentiate the performance particularly of the organomodified dispersions, nC1 and nC2.

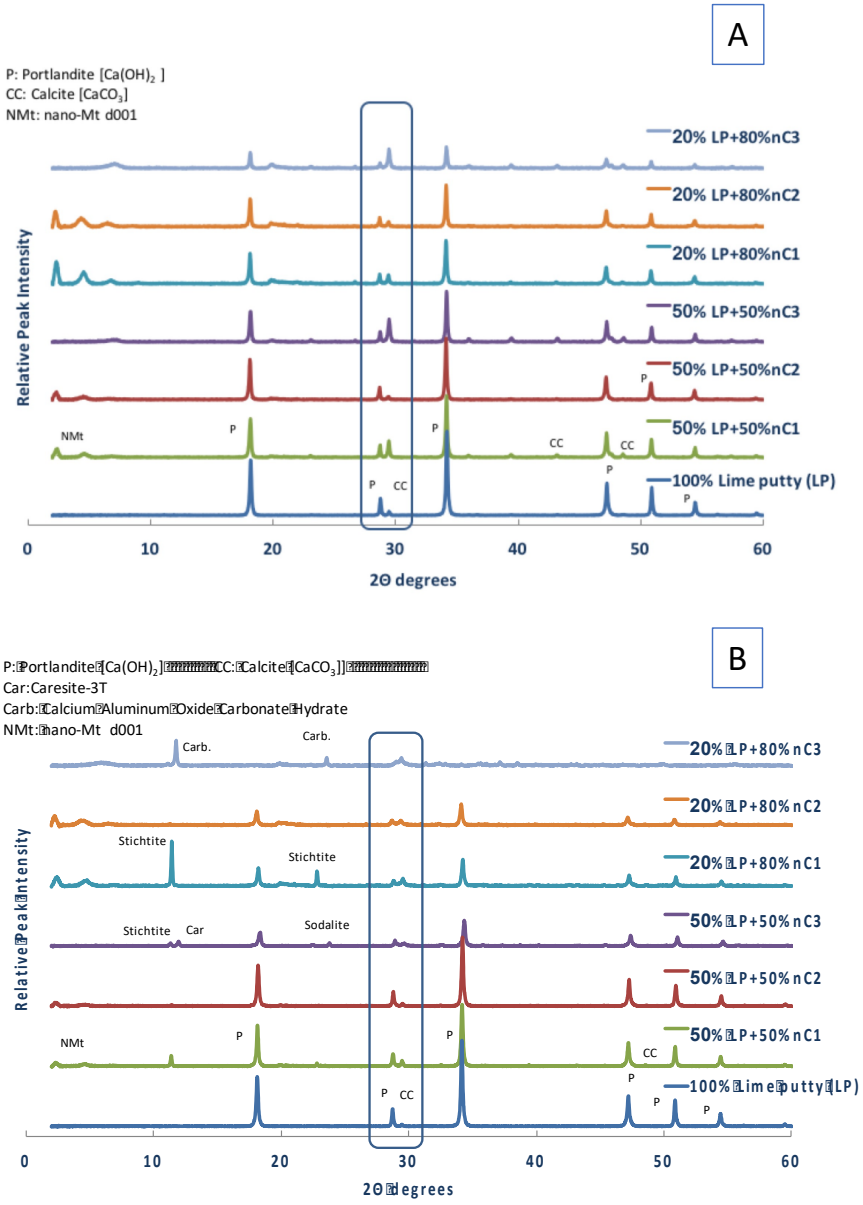


399

400 Figure 3: Investigation of pozzolanic activity: XRD analyses of LP/nC1, LP/nC2 and

401 LP/nC3 pastes (A) at day 8 and (B) at month 8

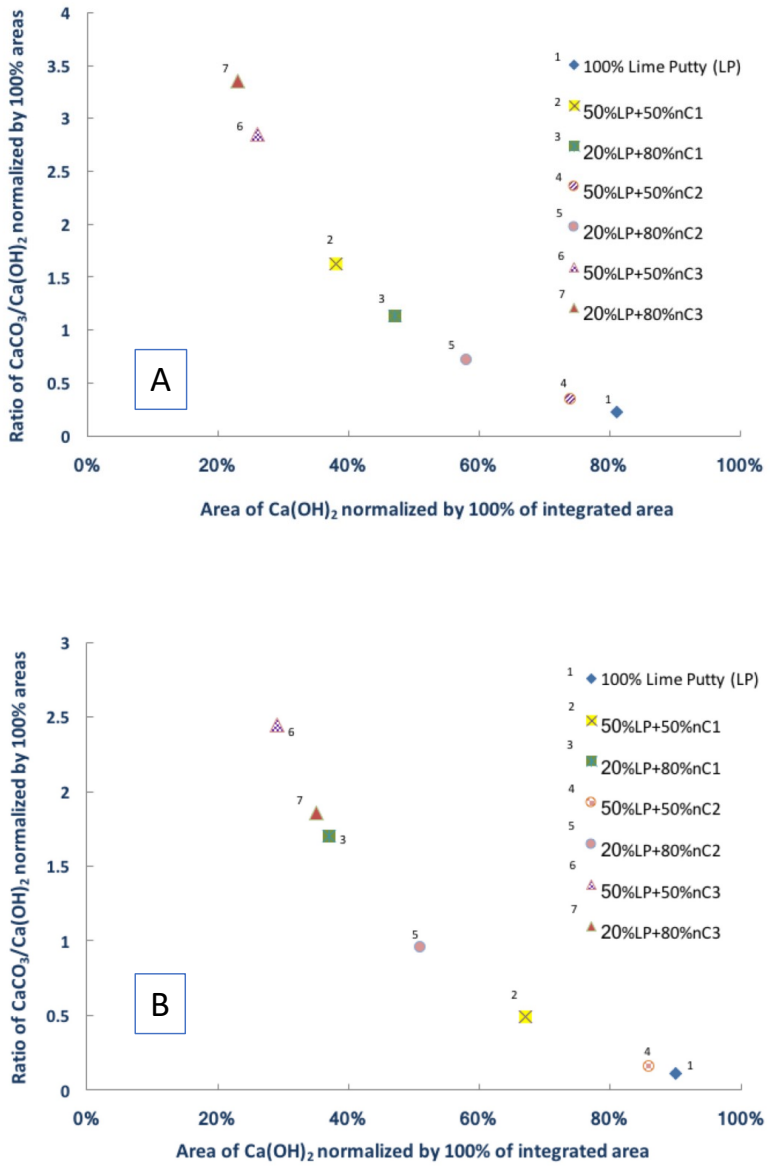


402

403 Figure 4: Results of semi-quantitative XRD analyses of LP/nC1, LP/nC2 and LP/nC3

404 pastes (A) at day 8 and (B) at month 8

405

## 2.3. Thermal gravimetry

First of all, the decomposition stages of lime putty were studied. Next, for the decomposition of the raw NMt dispersions data was derived from published research [9,10] and lastly, the decomposition of the NMt enhanced lime putty pastes was scrutinized and discussed.

(i) Decomposition of lime putty paste

All results shown correspond to pastes pre-dried at 60°C. Additionally, only the reference (pure LP) paste, was pre-dried at 60°C and at 100°C and thermogravimetrically analysed for comparison (Figure 5), as suggested by [23]. It was found that pre-drying LP at 100°C almost drained it from surface water, therefore the TGA showed marginal mass loss up to 100°C. However, slightly greater amount of surface water was lost up to 100°C on TGA for the lime putty pre-dried at 60°C, as expected. Most importantly, pre-drying at either temperature did not affect the detection of pure $Ca(OH)_2$ content with was found to reach almost 90% by mass. In agreement with the study of [23] in which, one-month old lime putty lost free and adsorbed water (3.5%) up to 300°C, the chemically bound water (21.5%) related to $Ca(OH)_2$ content up to 550°C and mass (2.3%) related to decomposition of $CaCO_3$ above 600°C, in this study the mass losses were recorded at similar temperature ranges and exhibited almost equal mass losses related to $Ca(OH)_2$ and $CaCO_3$ content, implying that the lime putty had slightly carbonated (Table 2).

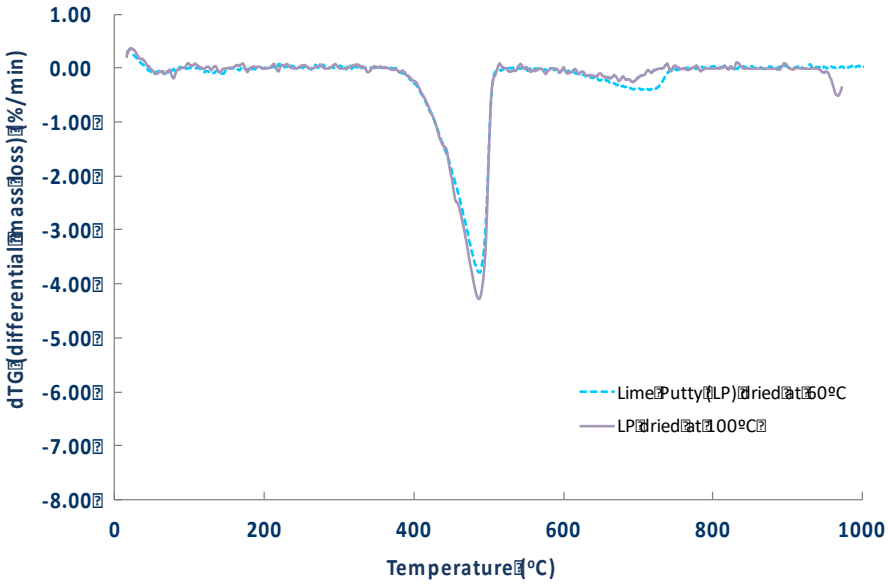


424

425 Figure 5: Comparison of dTG curves of LP dried at different temperatures

426

427 Table 2: dTG recorded mass loss (%) of lime putty

428

| Sample | 100-200°C | 200-300°C | 300-400°C | 400-600°C | 600-800°C | 800-1000°C |
|---|---|---|---|---|---|---|
| Dried 100% LP at day 8 | 0.33 | | 20.20 | | 3.52 | 0 |
| Dried 100% LP at month 8 | 0.33 | | 21.24 | | 1.62 | 0 |

429

430 **At day 8:**

431 (1) => $M_{CH}^{LP}$ = 20.2%, therefore following equation 3: $MM_{CH}^{LP}$ = 20.2/0.243 = 83.13

(2) => $M_{CC}^{LP}$ = 3.52%, therefore following equation 4: $MM_{CC}^{LP}$ = 3.52/0.44 = 8.0

$MM_{carbCH}^{LP}$ =$MM_{CC}$ / 1.35 = 8/1.35= 5.93

Following equation 5: $MM_{totCH}^{LP}$ = 83.13 + 5.93 = 89.06

Therefore, **for 50%LP: $MM_{totCH}^{LP}$ = 44.53 and for 20%LP: $MM_{totCH}^{LP}$ = 17.82**

**Accordingly, at month 8:**

(1) => $M_{CH}^{LP}$ = 21.2%, therefore following equation 3: $MM_{CH}^{LP}$ = 21.2/0.243 = 87.24

(2) => $M_{CC}^{LP}$ = 1.6%, therefore following equation 4: $MM_{CC}^{LP}$ = 1.6/0.44 = 3.7

$MM_{carbCH}^{LP}$ = $MM_{CC}$ / 1.35 = 3.7/1.35= 2.74

Following equation 5: $MM_{totCH}^{LP}$ = 87.24 + 2.74 = 89.98

Therefore, **for 50%LP: $MM_{totCH}^{LP}$ = 45.0 and for 20%LP: $MM_{totCH}^{LP}$ = 18.0**

(ii) Decomposition of raw nC1, nC2, nC3 dispersions

The qualitative interpretation of the decomposition stages of the three raw NMt dispersions is described in an earlier paper [10].

With respect to the organomodified NMt dispersions it is known that the modifier of the starting NMt powder (XDB) was intended to be fully decomposed by 500°C (resulting in a loss of 43% by mass, as mentioned in section 2.1.1 and 2.1.2). Three peaks are identified via differential thermal gravimetry analyses of nC1 and nC2 dispersions: (i) at 70°C, related to the loss of free water (ii) at 200°C assigned to the decomposition of the modifier and (iii) at 360°C assigned to loss of the modifier molecules physically adsorbed on the surface of the Mt layers with a

shoulder at around 410°C for nC1 or the main peak without any shoulders at 410°C for nC2, attributed to deconstruction of the modifier bound to the interlayer of the NMt [10].

In terms of quantitative analysis of the mass losses recored during the various temperature intervals, differential thermal gravimetry analysis of nC1 and nC2 dispersion yielded the following results [35]:

Table 3: dTG analysis recorded mass loss (%) of nC1 and nC2 dispersions

| **Sample** | **0-100°C** | **100-180°C** | **180-280°C** | **280-400°C** | **400-500°C** | **500-600°C** | **>600°C** |
|---|---|---|---|---|---|---|---|
| **Dried 100% nC1** | 0.68 | 2.63 | 6.73 | 35.34 | 9.48 | 2.17 | 0.00 |
| **Dried 100% nC2** | 1.02 | 1.82 | 6.52 | 25.95 | 20.14 | 2.29 | 0.00 |

It should be noted that for nC1 the mass loss between 280-500°C was equal to 44.8%, whilst for nC2 the mass loss between 280-500°C was equal to 46.1%. These were both slightly higher than the theoretical loss of mass of 43%. Moreover, there are traces of mass lost between 500-600°C. These mass losses can be attributed to the decomposition of the surfactants. For nC1 the surfactant and antifoam used is known to decompose below 400°C, whereas the surfactant used for nC2, the alkyl aryl sulphonate, is known to decompose at 580°C.

The inorganic dispersion nC3 exhibited different behaviour, therefore the thermal decomposition involved less stages than the organomodified dispersions (Table 5). Three peaks were present; one at 85°C with a shoulder at 110°C due to the loss of adsorbed water, a broader peak at 650°C and a sharp peak at 750°C which may be attributed to the loss of structural water

– dihydroxylation of the Mt. The complete deconstruction of the Mt (loss of 4% by mass) took place between 600-800°C as also reported in literature [6,36,37]. It should be noted, though, that the dispersant used for nC3, the tripolyphosphate, also decomposes at 600ºC [10].

Differential thermal gravimetry analysis of nC3 dispersion yielded the following mass losses [35]:

Table 4: dTG analysis recorded mass loss (%) of nC3 dispersion

| **Sample** | **0-100ºC** | **100-180ºC** | **180-300ºC** | **300-600ºC** | **600-800ºC** | **800-1000ºC** |
|---|---|---|---|---|---|---|
| **Dried 100% nC3** | 10.82 | 5.34 | 1.00 | 1.00 | 3.30 | 1.13 |

(iii) Decomposition of LP/nC1, LP/nC2 and LP/nC3 pastes

The pastes were thermogravimetrically analysed at 8 days and at 8 months (Figure 6). XRD analyses is required for the determination of the various compounds which decompose at similar temperature intervals.

For the temperature range between 20-100°C all free water was evaporated. For the temperature range between 110-400°C: The pozzolanic reaction between lime putty and NMt dispersions produced hydrates similar to the ones found in literature for lime/metakaolin pastes; calcium silicate hydrates (C–S–H), decomposing between 110-140°C, strätlingite ($C_2ASH_8$) decomposing between 140-200°C and $C_4ASH_{13}$ decomposing between 200-270°C and $C_3ASH_6$

490 decomposing between 270-380°C [38,39]. Indeed, strätlingite and other calcium-containing
491 hydrates were also confirmed in this research via XRD analysis.
492 Moreover hydrocalumite a carbonate compound traced via XRD in the 50%LP50%nC3-8
493 month-old paste, undergoes dihydroxylation between 200-400°C [40].
494 Furthermore, stichtite traced via XRD in the 50%LP50%nC1 and 20%LP80%nC1 -8 month-old
495 paste, and caresite-3T (another carbonate) traced via XRD in the 50%LP50%nC3-8 month-old
496 paste, also decomposed within this temperature range [41], although for stichtite other
497 researchers state 550 and 670°C as the main peaks signalling its decomposition [42].
498 Lastly, calcium aluminium oxide hydrate carbonate mainly decomposed between 180-280°C,
499 which justified the increased mass loss within this temperature range for the nC3 enhanced
500 pastes [33].
501
502 For the temperature range between 400-500°C the consumption of $Ca(OH)_2$ could not be clearly
503 observed in the early age thermograms at day 8, analytical elaboration was necessary. At month
504 8 all the higher nC content pastes showed pozzolanic reactivity. However, only the
505 20%LP+80%nC3 at month 8 clearly showed extinction of $Ca(OH)_2$ towards significant
506 production of hydrates (Figure 6 (D) to (F)). For the remaining pastes, including all early age
507 ones, judging whether $Ca(OH)_2$ was consumed or not was not obvious from the thermographs
508 because between 400-500°C two parts were decomposing towards the production of hydrates:

509 • nC1/nC2 dispersions (containing the modifier and Mt), which fully decomposed by
510 500°C
511 • and $Ca(OH)_2$

512 Moreover, although minor carbonation has taken place for the 8-month old samples as
513 witnessed by the endothermic peak present at approximately 730°C, the calculation of the
514 amount of $CaCO_3$ produced was intricate because above 600°C three parts were decomposing:

515 • nC3 containing the surfactant (tripolyphosphate) and Mt
516 • calcite typically traced in montmorillonites [9]
517 • and $CaCO_3$ due to the carbonation of $Ca(OH)_2$
518
519 For the temperature range above 800°C, no formation of high temperature silicate minerals e.g.
520 cristobalite, mullite or spinel was detected either at day 8 nor at month 8 via XRD analyses.
521 Other $CO_3$-containing compounds of the 8-month-old pastes were detected via XRD, such as
522 sodalite, which decomposes above 840°C [43] and calcium aluminium oxide hydrate carbonate
523 which decomposes above 800°C [33].
524
525 As a concluding remark the temperature range 400-500°C selected for assessing if $Ca(OH)_2$ was
526 consumed or not encompassed the decomposition of $Ca(OH)_2$ and nC1/nC2 and the temperature
527 range 600-800°C selected for recalculations for carbonation, encompassed the decomposition of
528 $CaCO_3$ (Mg-calcite and calcite) and nC3.

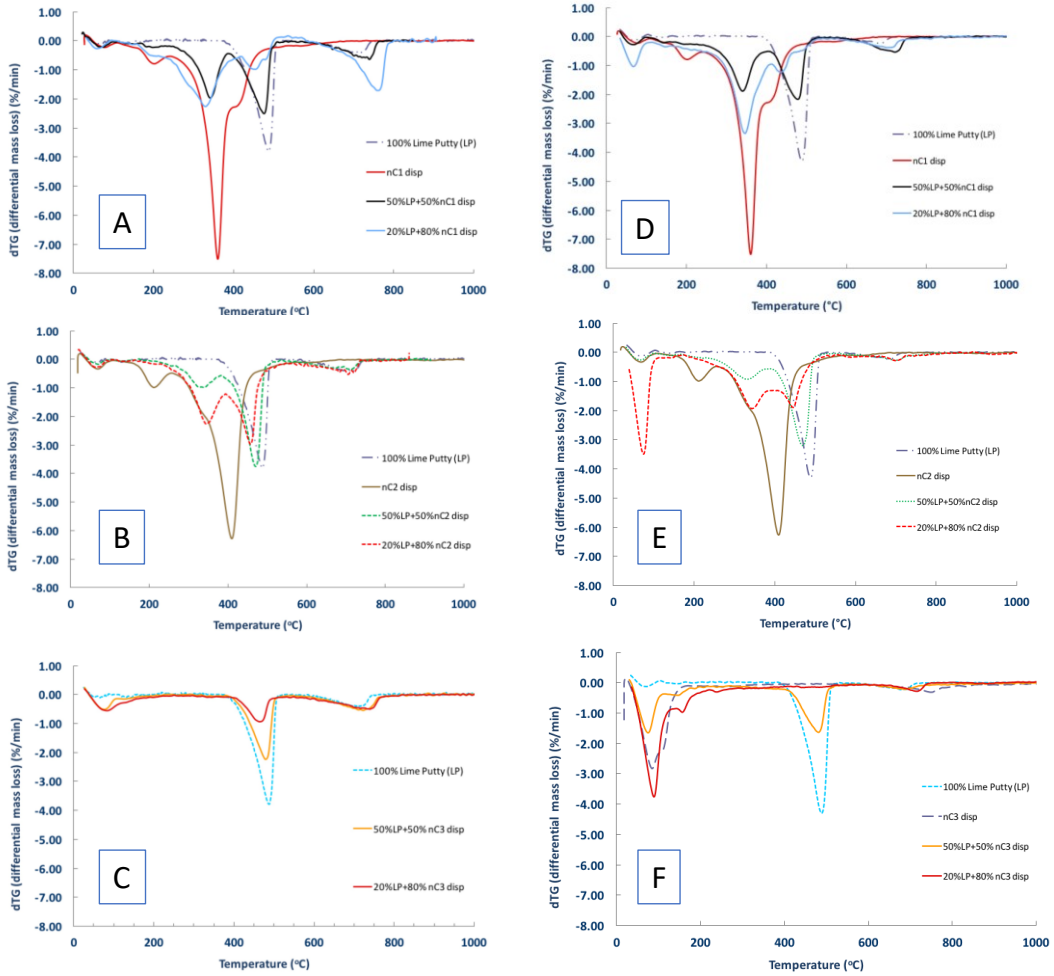


Figure 6: TGA for (A) LP/nC1, (B) LP/nC2, (C) LP/nC3 pastes at 8 days and (D) LP/nC1, (E) LP/nC2, (F) LP/nC3 pastes at 8 months

Table 5 and Table 7 contain the exact mass loss of the LP/nC pastes recorded at the various temperature intervals, by the TG analyser. For the net amount of $Ca(OH)_2$ consumed up to 500°C, the amount of nC1, nC2 or nC3 present must be deducted from the mass loss recorded by the TG analyser (Table 5 and Table **7**) for the decomposition of the NMt enhanced lime putty pastes within the specific temperature range.

Respectively, for the net amount of $CaCO_3$ detected due to carbonation of a part of $Ca(OH)_2$ the amount of nC3 decomposing between 600-800°C must be deducted from the mass loss recorded by the TG analyser (Table 5 and Table **7**) within the specific temperature range.

Table 5: dTG recorded mass loss (%) of LP/nC1, LP/nC2 and LP/nC3 pastes - at day 8

| **Sample** | **0-100°C** | **100-200°C** | **200-300°C** | **300-400°C** | **400-500°C** | **500-800°C** | **800-1000°C** |
|---|---|---|---|---|---|---|---|
| Dried 50% LP + 50% nC1 | 0.64 | 1.06 | 2.8 | 10.53 | 13.97 | 5.93 | 0 |
| Dried 50% LP + 50% nC2 | 0.36 | 0.20 | 2.04 | 7.35 | 18.63 | 4.19 | 0 |
| Dried 50% LP + 50% nC3 | 2.34 | 0.60 | 0.56 | | 8.88 | 11.73 | 0 |
| Dried 20% LP + 80% nC1 | 0.21 | 1.68 | 8.72 | 14.29 | 12.72 | 12.34 | 0 |
| Dried 20% LP + 80% nC2 | 0.74 | 0.46 | 3.30 | 15.54 | 16.11 | 6.46 | 0 |
| Dried 20% LP + 80% nC3 | 4.13 | 2.34 | 0.83 | | 3.60 | 9.00 | 0 |

Estimating the theoretical mass loss related to the CH required analytical calculations, presented in the appendix for the ease of the reader. The results of these calculations are compared to the recorded values by the TGA Table 6. Theoretical and experimental values corroborated well at 8 days. The first column of Table 6 presents the results of $M_{CH}$ of the Appendix table 2. The second column of Table 6 contains the recordings for temperature range 400-500°C presented in Table 5.

Table 6: Theoretical and experimental mass loss (%) of LP/nC1, LP/nC2 and LP/nC3 pastes related to CH consumption - at day 8

| **Sample** | Theoretically expected mass loss (%) | Experimentally attained (TGA) mass loss (%) | Mass loss reduction related to CH consumption |
|---|---|---|---|
| 50%LP+50%nC1 | 14.8 | 13.97 | 5.6% |
| 50%LP+50%nC2 | 20.2 | 18.63 | 7.8% |
| 50%LP+50%nC3 | 10.6 | 8.88 | 16% |
| 20%LP+80%nC1 | 11.6 | 12.72 | - |
| 20%LP+80%nC2 | 20 | 16.11 | 20% |
| 20%LP+80%nC3 | 4.8 | 3.60 | 25% |

552 Similarly, the experimental mass losses recorded at the different temperature intervals for the 8-
553 month-old pastes are presented in Table **7** and the theoretical mass loss related to the CH
554 (analytically calculated in the appendix) are presented in

555

556

557 Table **8**. Theoretical and experimental values corroborated well for the 50%Lp and 50% nC1 or
558 nC2 or nC3 dispersions. at 8 months. For the higher NMt content combinations, the
559 experimentally attained mass loss (by the TGA/dTG) was significantly greater than the
560 theoretically expected. This could indicate a significant pozzolanic activity with increased NMt
561 quantities, given the time. In fact, at approximately 275ºC and above 455ºC dehydroxylation of
562 stichtite and caresite which were previously detected via XRD at the 8 months old samples,
563 occurs [44]. Hydrocalumite also decomposes within 400-500ºC [40]. Lastly, calcium aluminate
564 carbonate hydrates decompose mostly at 220 ºC and 260 ºC [33].

565

566 Table 7: dTG recorded mass loss (%) of LP/nC1, LP/nC2 and LP/nC3 pastes at month 8

| **Sample** | **0-100ºC** | **100-200ºC** | **200-300ºC** | **300-400ºC** | **400-500ºC** | **500-800ºC** | **800-1000ºC** |
|---|---|---|---|---|---|---|---|
| Dried 50% LP + 50% nC1 | 0.83 | 1.55 | 3.71 | 10.93 | 12.47 | 5.57 | 0 |
| Dried 50% LP + 50% nC2 | 0.81 | 0.76 | 2.86 | 6.90 | 17.26 | 3.40 | 0 |
| Dried 50% LP + 50% nC3 | 5.43 | 2.38 | 2.66 | | 9.23 | 2.94 | 0.34 |
| Dried 20% LP + 80% nC1 | 3.46 | 2.70 | 5.81 | 20.68 | 8.10 | 5.50 | 0 |
| Dried 20% LP + 80% nC2 | 10.18 | 1.45 | 4.34 | 14.46 | 11.37 | 4.93 | 0 |
| Dried 20% LP + 80% nC3 | 13.45 | 6.65 | 3.96 | | 1.42 | 3.00 | 0 |

567

568

569

570 Table 8: Theoretical and experimental mass loss (%) of LP/nC1, LP/nC2 and LP/nC3

571 pastes related to CH consumption - at month 8

| **Sample** | Theoretically expected mass loss (%) | Experimentally attained (TGA) mass loss (%) | Mass loss reduction related to CH consumption |
|---|---|---|---|
| 50%LP+50%nC1 | 15.4 | 12.5 | 19% |
| 50%LP+50%nC2 | 20.7 | 17.3 | 16.% |
| 50%LP+50%nC3 | 11.1 | 9.3 | 16.8% |
| 20%LP+80%nC1 | 11.8 | 8.1 | 31.4% |
| 20%LP+80%nC2 | 20.4 | 11.4 | 44.3% |
| 20%LP+80%nC3 | 5 | 1.4 | 71.6% |

572

573 Deducting the mass loss related to the Mt decomposition from the mass loss recorded by the TG
574 analyser required analytical calculations, presented in the appendix for the ease of the reader.
575 The results of these calculations in terms of mass loss and molar mass are introduced in Table 9
576 and

577 Respectively, the experimental $MM_{totCH}$ is given in the appendix, Table Ap-3. The theoretical
578 $MM_{totCH}$ is given in the appendix, Table Ap-4.

579 Table 10. The experimental $MM_{totCH}$ is given in the appendix, Table Ap-1. The theoretical
580 $MM_{totCH}$ is given in the appendix, Table Ap-2.

581

582 Table 9: Results of mass loss and total molar mass of CH ($MM_{totCH}$) [equation 1-5] at day 8

| **Sample** | Experimental $MM_{totCH}$ **Eq5** | CRITERION | Theoretical $MM_{totCH}$ | Pozzolanic behaviour [Yes (Y)/No (Y)/ equal (=)] |
|---|---|---|---|---|
| **50%LP+50%nC1** | 47.85 | < | 60.91 | Y |
| **50%LP+50%nC2** | 42.44 | < | 83.13 | Y |

| | | | | |
|---|---|---|---|---|
| **50%LP+50%nC3** | 50.56 | = | 50.32 | = |
| **20%LP+80%nC1** | 40.17 | < | 47.74 | Y |
| **20%LP+80%nC2** | 10.94 | < | 82.30 | Y |
| **20%LP+80%nC3** | 20.78 | < | 26.75 | Y |

583

584 Respectively, the experimental $MM_{totCH}$ is given in the appendix, Table Ap-3. The theoretical
585 $MM_{totCH}$ is given in the appendix, Table Ap-4.

586 Table 10: Results of mass loss and total molar mass of CH ($MM_{totCH}$) [equation 1-5] at month 8

| **Sample** | Experimental $MM_{totCH}$ **Eq5** | CRITERION | Theoretical $MM_{totCH}$ | Pozzolanic behaviour [Yes (Y)/No (Y)/equal (=)] |
|---|---|---|---|---|
| **50%LP+50%nC1** | 41.18 | < | 63.37 | Y |
| **50%LP+50%nC2** | 35.31 | < | 85.19 | Y |
| **50%LP+50%nC3** | 37.16 | < | 52.41 | Y |
| **20%LP+80%nC1** | 11.39 | < | 48.56 | Y |
| **20%LP+80%nC2** | 8.29 | < | 83.95 | Y |
| **20%LP+80%nC3** | 2.55 | < | 27.65 | Y |

587

588 From the elaboration presented above, the complexity of assessing the pozzolanic potentials of
589 LP/nC1 or LP/nC2 or LP/nC3 pastes is demonstrated and resolved. It can be interpreted from
590 the TG analyses that the higher NMt concentrations at 8 months can lead to the elimination of
591 $Ca(OH)_2$ and that in all cases nC3 showed the highest pozzolanic activity, followed by nC2.
592 With respect to the comparison between the performance of nC1 and nC2, it can be claimed that
593 the better dispersed NMt particles, nC2, as tested by TGA, XRD and transmission electron
594 microscopy imaging and crystallographic analyses [10] seem to be developing more stable
595 bonds when participating in hydration reactions. The bulk of the material decomposes at higher
596 temperature ranges (over 400°C) than nC1, which starts to decompose at 300°C. Possibly, the
597 carbon molecules inserted within the platelets of nC2 that were intended to keep them apart did

598 not function as such, avoiding re-agglomeration of the NMt platelets. Furthermore, they
599 possibly prevented carbonates from forming, as the LP/nC2 pastes did not show signs of
600 carbonation at either age. On the contrary, the NMt particles of nC1, which by the
601 abovementioned materials characterization techniques were found to be re-agglomerating and
602 covered in an excess of organic matter [10], exhibited less stable bonds, decomposing at a lower
603 temperature band and engaged in carbonation reactions with various carbonaceous compounds
604 being formed.

605 **2.4. XRD analyses of raw NMt and Chapelle products**

606 The pozzolanic activity of the samples was confirmed by XRD analyses of the raw powders [9]
607 XDB (Figure 7A) and HPS (Figure 7E) compared with their Chapelle products Chap-XDB
608 (Figure 7B) and Chap-HPS (Figure 7F). Most importantly the XRD analyses of the raw NMt
609 dispersions [10] nC2 (Figure 7C) and nC3 (Figure 7G) compared with their Chapelle products
610 Chap-nC2 (Figure 7D) and Chap-nC3 (Figure 7H), are also presented. To the best knowledge of
611 the authors this is the first time that the Chapelle method was used for testing the pozzolanic
612 activity of non-calcined nano-montmorillonite dispersions. The following phases were identified
613 in the raw dispersions: montmorillonites and feldspars for nC2 (Figure 7C) and sodium calcium
614 magnesium aluminum silicate hydrate, sodium aluminum silicate hydroxide, calcite and
615 feldspars for nC3 (Figure 7G). The reaction of 1 g of nC dispersion with 1 g of $Ca(OH)_2$ and
616 100 ml of boiled water yielded sodium calcium magnesium aluminum silicate hydrate and
617 calcite for Chap-nC2 (Figure 7D) and calcium aluminum silicate hydroxide (CASH)/katoite and
618 saponite for Chap-nC3 (Figure 7H). Both CASH and katoite (a low silica hydrogarnet) have
619 been identified as products of pozzolanic reactions under hydrothermal conditions [45,46].
620 Furthermore, according to Gameiro et al who also traced katoite in their lime-metakaolin
621 mortars, they concluded that this phase decreases together with calcium hydroxide as the age of

622 the mortar advances [47]. More importantly, it has been postulated that katoite is more resistant
623 to carbonation than other salts formed during pozzolanic reactions [48]. Lastly, it is worth
624 noting that the nano-montmorillonite dispersions bear significant resemblance to the starting
625 powders they emerged from. Therefore, the nano-montmorillonite and montmorillonite,
626 feldspar, calcite and quartz detected in XDB (Figure 7A) produced a significant amount of
627 calcite and sodium calcium magnesium aluminum silicate hydrate under the Chapelle test
628 (Figure 7B). In fact, this result is in absolute accordance with studies on nC2 modified
629 composite cement formulations, in which significant amounts of calcite were traced via XRD
630 and thermal-gravimetric analyses [8]. This is one of the main reasons for which the
631 organomodified nano-montmorillonite dispersions have been found less favourable when added
632 to cement pastes. On the contrary, the inorganic montmorillonite HPS which contained
633 montmorillonite, calcite, quartz, feldspar and magnesium aluminium silicates (Figure 7E) also
634 reacted with $Ca(OH)_2$ in boiled water, producing ample CASH and katoite, clearly showing that
635 the inorganic montmorillonite, be it raw or dispersed, has pozzolanic properties.

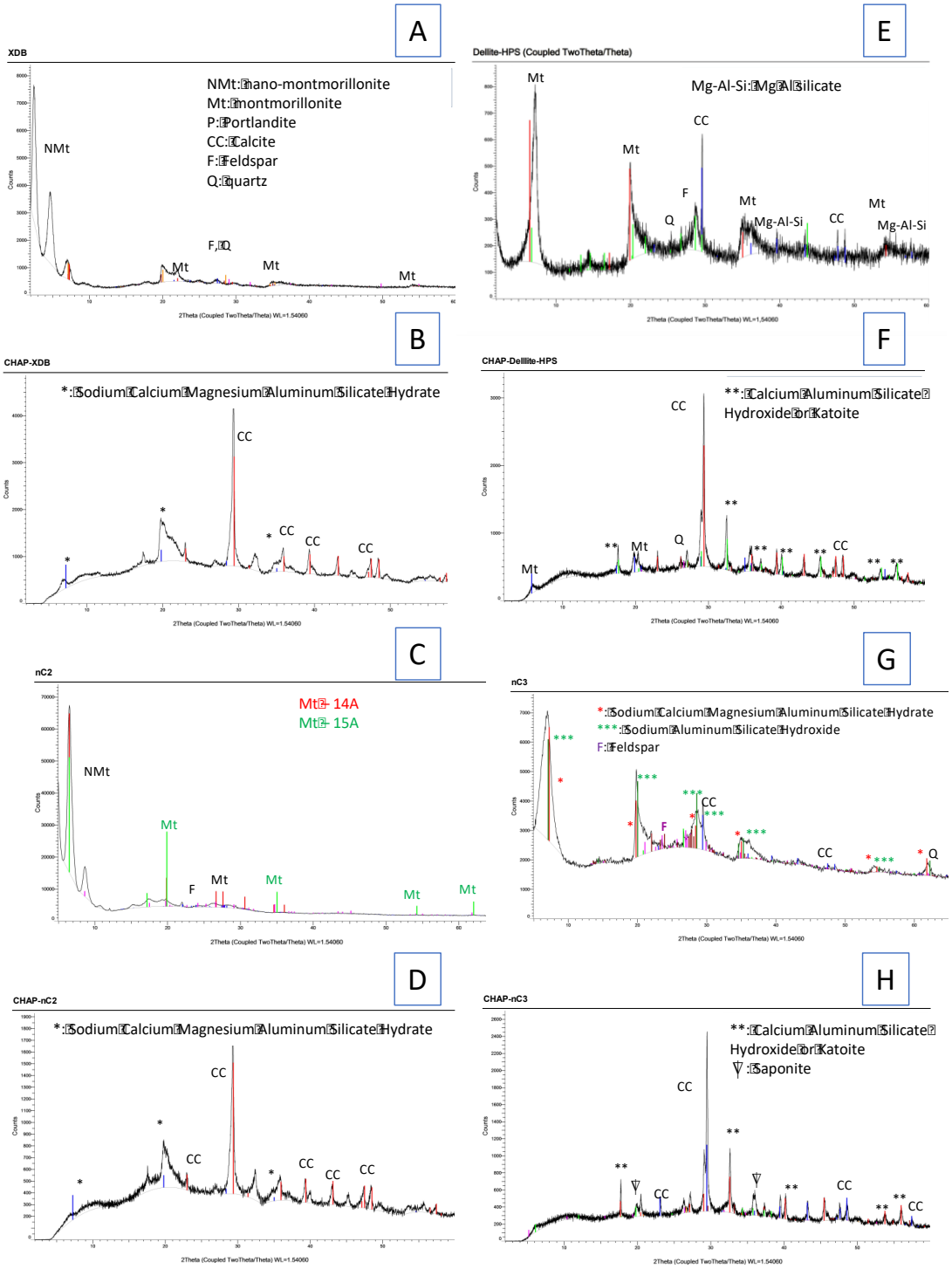


636

637 Figure 7: XRD for (A) XDB, (B) Chapelle-XDB, (C) nC2 , (D) Chapelle-nC2, (E) HPS,

638 (F) Chapelle-HPS, (G) nC3, (H) Chapelle-nC3

## 3. Discussion

Lime putty, rich in $Ca(OH)_2$ is a traditional building material used for centuries and still preferred to date for historic building conservation [24] particularly against Portland cement which is found in many cases highly incompatible with historic lime mortar masonry monuments [22]. However, current codes require that existing masonry structures must be retrofitted in order to withstand a combination of loads, for which increased mortar strength may offer a partial retrofitting upgrade. Given that Portland cement is avoided in historic mortar conservation, nano-montmorillonite could be used as an alternative binding pozzolanic and nanostructural reinforcing agent. Furthermore, NMt dispersions comprise even more interesting nanoreinforcement as they are easier to handle and can be more homogeneously dispersed in binders. In addition, the irreversible colloidal behaviour of lime putty has been linked to the oriented aggregation occurring during drying of the lime putty. While transmission electron microscopy imaging and crystallography support this finding, field emission scanning electron microscopy has also revealed plate-like nanoparticles of $Ca(OH)_2$ clustering up to micron-sized elements. Slaked lime putty is, therefore, postulated to be compatible in terms of micro and nanostructure with NMt particles, which when dispersed comprise of nano-thick platelets individually available for reactions [4,10].

Recently published research conducted by the authors, on the nanostructure of the NMt dispersions [10] and characterization via TEM imaging and crystallography, XRD, SEM/EDX and TGA/DTG also taking into consideration results published in cement pastes [8] revealed that in nC1 the platelets were not fully exfoliated, and were possibly re-agglomerating in cement paste. This re-agglomeration increased the size of the particles to the micro-level, creating voids and allowing cracks to easily propagate in the hydrating cement pastes. It was concluded that

662 the surfactant used in this dispersion rendered the resulting pastes less resistant in both tension
663 and compression.

664 With respect to nC2, platelets were found to be partially exfoliated, with several platelets
665 intercalated in the volume of the dispersion. Overall, NMt platelets were better dispersed in
666 water with the use of the anionic surfactant [10], which also significantly affected the
667 mechanical performance of the nC2 enhanced Portland-limestone pastes [8]. It was concluded
668 that the higher energy bonds between the NMt platelets and the anionic surfactant kept the
669 platelets apart, while not allowing their slippage and crack evolution. A tortuous crack pattern,
670 was developed, leading to more ductile behaviour and flexural strength improvements, still
671 presenting areas of weakness due to some agglomeration of particles.

672 Lastly, the nanostructure of nC3 revealed exfoliated platelets, well dispersed in the volume of
673 the paste acting as nanoreinforcement having potentials for seeding agent action. Better particle
674 packing and increased platelets specific surface area was achieved in nC3, with NMt platelets
675 playing the role of nanofillers. This configuration also allowed for significant inhibition of crack
676 development, favouring flexural strength development and less brittle performance when added
677 in binders.

678 In this research, these three different NMt dispersions were investigated in NMt/lime putty
679 pastes with respect to their pozzolanic potentials. It can be claimed overall that the complex
680 chemistry involved in the production of organomodified NMt dispersions affected not only their
681 nanostructure as postulated by earlier studies [10] but also their pozzolanic performance.
682 Adding to this, the type of surfactant or the amount of modifier present is setting a threshold on
683 the allowable amount of NMt in lime putty or even cement pastes. In other words, it is possible
684 that the organomodification process either due to the high amount of carbon present in the
685 modifier or due to the alteration of the platelet surface charge, depending on the type of

686 surfactant used, is not allowing nC1 nanoplatelets and some of nC2 nanoplatelets to act as
687 nucleation agents for reactions. The quaternary ammonium salts introduced in the galleries of
688 the organomodified NMt as well as the surfactants employed for dispersing the platelets
689 differentiate the chemical bond strength leading to lower energy formations for nC1 but
690 maintaining the higher energy bonds found in the raw dispersions [10], in the NMt/lime patty
691 pastes also for nC2 (Figure 8 (A) and(B)). This is the reason why the thermal gravimetric
692 analyses of the LP/nC1 and LP/nC2 pastes differ, although the starting NMt powder was the
693 same. nC1, which showed the poorest nanostructure, still exhibited some pozzolanic activity
694 although this was challenged by the high amounts of carbon present in the sample and the re-
695 agglomeration of the platelets. nC2, showed pozzolanic activity, increasing with curing age and
696 higher proportions of nC2. nC3 exhibited the highest and most rapid consumption of $Ca(OH)_2$
697 towards production of calcium silicate and/or calcium aluminate hydrates possibly due to its
698 simpler chemistry and nanostructure. The exfoliated platelets must have been individually
699 reactive, engaging in pozzolanic reactions as seeding agents and catalysts (Figure 8 (C)).

700 Overall, the pozzolanic activity in terms of $Ca(OH)_2$ consumption was more pronounced for the
701 better dispersed NMt particles (nC2 and nC3). A qualitative interpretation of the TGA results
702 shown is that both nC1 and particularly nC2 dispersions are forming new more thermally stable
703 bonds in presence of $Ca(OH)_2$ signalled by the new peaks at about 435°C. In fact, all LP/nC1
704 and LP/nC2 pastes exhibit a two-stage decomposition with two distinct peaks at 385°C and at
705 435°C, however the mass losses related to the peaks, shift depending on the NMt dispersion
706 content. Therefore, the accuracy of the criterion could be challenged if the temperature range for
707 the $Ca(OH)_2$ consumption detection is broadened. However, the temperature range 400-500°C
708 selected for the criterion offers a good approximation. For this, it was postulated that inorganic
709 NMt dispersions, show more distinct performance in terms of $Ca(OH)_2$ consumption detection.

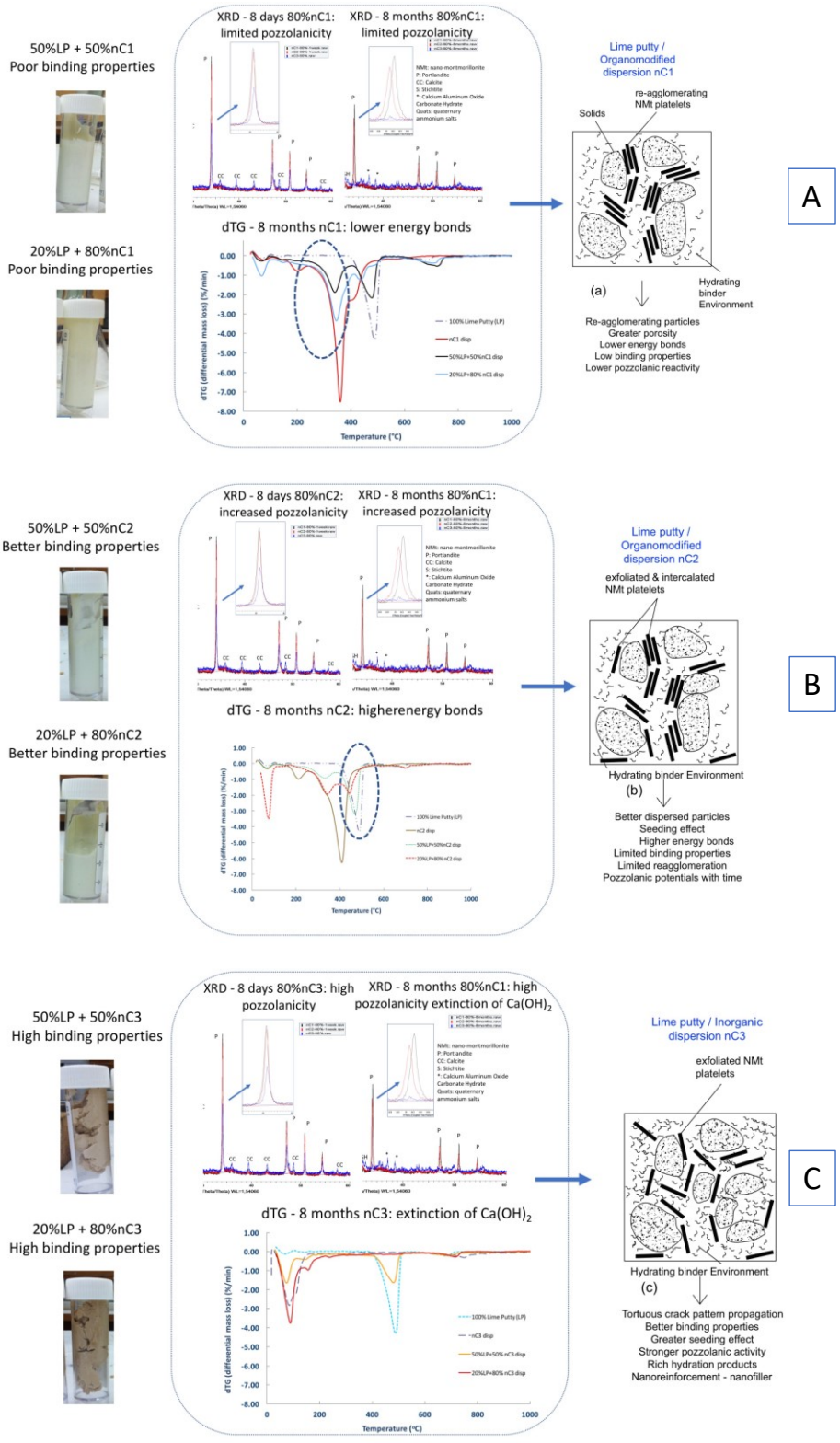


710

711 Figure 8: Binding properties, TGA and XRD related to nanostructure of (A) LP/ nC1, (B)

712 LP/ nC2 and (C) LP/ nC3 pastes

713 Furthermore, knowing that the average amorphous Si/Al ratio of nC1 is 4.23, nC2 is 4.08 and
714 nC3 is 2.71 [10], all three dispersions can be expected to consume $Ca(OH)_2$ and form calcium
715 silicate and/or calcium aluminate hydrates. Indeed, it can be argued that nC1 and nC3 produced
716 more C–S–H, although it is acknowledged that molar calculations are difficult in this region due
717 to the simultaneous decomposition of the modifier for nC1. Still, the carbonated hydrates traced
718 in the 8-month-old LP/nC3 pastes reinforce this hypothesis.
719 These results presented herein are in agreement with results presented in NMt enhanced cement
720 pastes. Extensive TG analyses on NMt enhanced cement pastes [8], suggest that blended cement
721 pastes containing nC3 (ternary pastes of Portland cement, limestone and NMt) exhibited greater
722 consumption of $Ca(OH)_2$ towards the production of additional C–S–H and ettringite, while nC1
723 and nC2 showed similar C–S–H and ettringite production until day 90.

724 It has been suggested the second derivate of thermogravimetric curve (DDTG) gives new
725 possibilities for detailed investigations of overlapping decomposition mass losses [44], however
726 the advanced mathematical elaboration involved [49] would only add to the already high level
727 of inherent complexity and for this, such calculations were not considered in this research.

728 Further investigation of the LP/nC1 or LP/nC2 or LP/nC3 pastes would have provided visual
729 representation of the pastes produced. For instance, scanning electron microscopy studies would
730 have revealed agglomerated and hydrated particles. However, this was not considered necessary
731 for the purpose of this paper, which was purely to device a criterion by which the pozzolanic
732 behaviour would be assessed in the complex matrix produced with the use of NMt. In fact, the
733 already existing test methods, namely the Chapelle method, Fratinni method and Strength
734 Activity Index have only been employed for the characterisation of calcined clays or cement
735 pastes. The validity of the Chapelle method has been questioned for any other materials.
736 Furthermore, due to the complex nature of the NMt dispersions, a new method should be

devised allowing for the quantification of the calcium hydroxide consumption. Although the mathematical elaboration of the results is not straightforward, still, the new method is offering more and in-depth information about the systems characterized. Lastly, given the assumptions made, the accuracy of the criterion was maintained.

The criterion of the new method was verified through a two-step process; (i) with respect to a theoretical estimation of the mass losses related to $Ca(OH)_2$ consumption and (ii) with respect to the net mass assigned to $Ca(OH)_2$ mathematically elaborated from the experimentally recorded value. It was also reinforced via XRD mineralogical analysis, as well as semi-quantitative analysis. Therefore, given the elemental composition of the NMt dispersions, TGA and XRD can be adequately combined to assess the pozzolanic behaviour of LP/nC1 or LP/nC2 or LP/nC3 pastes. The criterion was lastly validated via XRD analyses of the Chapelle products.

## 4. Conclusions

All things considered, primarily the nature (inorganic or organomodified) of NMt and the different dispersing agents both affect the thermal characteristics of NMt dispersions. For the first time, it was demonstrated that non-thermally treated Mt, nanomodified with the help of dispersion agents, can be potentially implemented in cementitious binders as a low carbon footprint, nanosized supplementary cementitious nanomaterial. Furthermore, a method for assessing the pozzolanic reactivity was devised, which allows for sound conclusions to be made, while simultaneously the Chappelle method was applied for the first time in (non-thermally treated) NMt dispersions. This research can provide a basis for the study of restoration pastes for superior properties. Therefore, the next generation of high performance materials produced via the manipulation of the size and distribution at the micro [47] and nano

level [48] is currently being studied and is expected to provide materials scientists and the engineering world with more sustainable options for the built environment.

To sum up, this study has:

- Devised a new criterion to assess the pozzolanic potential of NMt dispersions for use as supplementary cementitious materials through the study of NMt enhanced lime putty pastes.
- Applied Chapelle tests to (non-thermally treated) NMt dispersions for the first time, and results correlated well with the new method developed.
- Quantified the difference in pozzolanic reactivity of organomodified and inorganic NMt dispersions.
- Provided knowledge of the NMt surfactant decomposition stages and nanostructure that is essential for the interpretation of TG analysis of NMt enhanced lime putty pastes.
- Demonstrated that inorganic NMt dispersions exhibited rapid and pronounced pozzolanic activity signalling potential for advanced mechanical performance.
- Created a route for use of inorganic NMt dispersions in the production of lower carbon footprint cement binders as well as lime mortars for conservation of historic monuments.

## 5. Acknowledgements

The authors acknowledge the European Commission funding (FIBCEM project, grant Number 262954) and all partners are thanked for their input and for the supply of materials. The authors would also like to acknowledge the Department of Chemical Engineering at the University of Bath for the use of the TG analyser. Dr G.L. Pesce, University of Northumbria and. R.J. Ball,

University of Bath are thanked for scientific discussions. Moreover, the authors would like to thank the School of Chemical Engineering, at the Technical University of Athens (NTUA). Lastly, the authors acknowledge the Greek Ministry of Culture, Directorate of Restoration of Medieval and Post-Medieval Monuments, Department of Technical Research on Restoration for the use of the XRD software and for technical discussions.

## 6. References

[1] H. Dalir, R.D. Farahani, V. Nhim, B. Samson, M. Levesque, D. Therriault, Preparation of highly exfoliated polyester-clay nanocomposites: process-property correlations, Langmuir. (2012).

[2] R. Fernandez, F. Martirena, K.L. Scrivener, The origin of the pozzolanic activity of calcined clay minerals: A comparison between kaolinite, illite and montmorillonite, Cem. Concr. Res. 41 (2011) 113–122. doi:http://dx.doi.org/10.1016/j.cemconres.2010.09.013.

[3] P.C. LeBaron, Z. Wang, T.J. Pinnavaia, Polymer-layered silicate nanocomposites: an overview, Appl. Clay Sci. 15 (1999) 11–29.

[4] S. Papatzani, Effect of nanosilica and montmorillonite nanoclay particles on cement hydration and microstructure, Mater. Sci. Technol. 32 (2016) 138–153. doi:10.1179/1743284715Y.0000000067.

[5] L.B. De Paiva, A.R. Morales, F.R. Valenzuela Díaz, Organoclays: properties, preparation and applications, Appl. Clay Sci. 42 (2008) 8–24.

[6] A. Vazquez, M. López, G. Kortaberria, L. Martín, I. Mondragon, Modification of montmorillonite with cationic surfactants. Thermal and chemical analysis

including CEC determination, Appl. Clay Sci. 41 (2008) 24–36. doi:http://dx.doi.org/10.1016/j.clay.2007.10.001.

[7] C.B. Hedley, G. Yuan, B.K.G. Theng, Thermal analysis of montmorillonites modified with quaternary phosphonium and ammonium surfactants, Appl. Clay Sci. 35 (2007) 180–188. doi:http://dx.doi.org/10.1016/j.clay.2006.09.005.

[8] S. Papatzani, K. Paine, Dispersed Inorganic or Organomodified Montmorillonite Clay Nanoparticles for Blended Portland Cement Pastes: Effects on Microstructure and Strength, in: K. Sobolev, S.P. Shah (Eds.), Nanotechnol. Constr. Proc. NICOM5, Springer International Publishing, 2015: pp. 131–139. doi:10.1007/978-3-319-17088-6_16.

[9] J. Calabria-Holley, S. Papatzani, B. Naden, J. Mitchels, K. Paine, Tailored montmorillonite nanoparticles and their behaviour in the alkaline cement environment, Appl. Clay Sci. 143 (2017) 67–75. doi:http://dx.doi.org/10.1016/j.clay.2017.03.005.

[10] S. Papatzani, K. Paine, Inorganic and organomodified nano-montmorillonite dispersions for use as supplementary cementitious materials - A novel theory based on nanostructural studies, Nanocomposites. 3 (2017) 2–19. doi:10.1080/20550324.2017.1315210.

[11] M. Fitos, E.G. Badogiannis, S.G. Tsivilis, M. Perraki, Pozzolanic activity of thermally and mechanically treated kaolins of hydrothermal origin, Appl. Clay Sci. 116–117 (2015) 182–192. doi:http://dx.doi.org/10.1016/j.clay.2015.08.028.

[12] G. Kakali, T. Perraki, S. Tsivilis, E. Badogiannis, Thermal treatment of kaolin: the effect of mineralogy on the pozzolanic activity, Appl. Clay Sci. 20 (2001) 73–80. doi:http://dx.doi.org/10.1016/S0169-1317(01)00040-0.

[13] N. Farzadnia, A.A. Abang Ali, R. Demirboga, M.P. Anwar, Effect of halloysite

nanoclay on mechanical properties, thermal behavior and microstructure of cement mortars, Cem. Concr. Res. 48 (2013) 97–104. doi:http://dx.doi.org/10.1016/j.cemconres.2013.03.005.

[14] C. He, E. Makovicky, B. Osbaeck, Thermal treatment and pozzolanic activity of Na- and Ca-montmorillonite, Appl. Clay Sci. 10 (1996) 351–368. doi:http://dx.doi.org/10.1016/0169-1317(95)00037-2.

[15] M. Aly, M.S.J. Hashmi, A.G. Olabi, M. Messeiry, A.I. Hussain, Effect of nano clay particles on mechanical, thermal and physical behaviours of waste-glass cement mortars, Mater. Sci. Eng. A. 528 (2011) 7991–7998. doi:10.1016/j.msea.2011.07.058.

[16] A. Hakamy, F.U.A. Shaikh, I.M. Low, Characteristics of nanoclay and calcined nanoclay-cement nanocomposites, Compos. Part B Eng. 78 (2015) 174–184. doi:https://doi.org/10.1016/j.compositesb.2015.03.074.

[17] A. Heath, K. Paine, S. Goodhew, M. Ramage, M. Lawrence, The potential for using geopolymer concrete in the UK, Proc. Inst. Civ. Eng. Constr. Mater. 166 (2013) 195–203.

[18] R. Kalpokaitė-Dičkuvienė, I. Lukošiūtė, J. Čėsnienė, K. Brinkienė, A. Baltušnikas, Cement substitution by organoclay – The role of organoclay type, Cem. Concr. Compos. 62 (2015) 90–96. doi:10.1016/j.cemconcomp.2015.04.021.

[19] British Standards Institution, BS EN 459-1. Building lime. Definitions, specifications and conformity criteria, UK, 2015.

[20] J. Pontes, A. Santos Silva, P. Faria, Evaluation of Pozzolanic Reactivity of Artificial Pozzolans, Mater. Sci. Forum. 730–732 (2013) 433–438. doi:10.4028/www.scientific.net/MSF.730-732.433.

[21] R. Giorgi, M. Ambrosi, N. Toccafondi, P. Baglioni, Nanoparticles for Cultural

854 Heritage Conservation: Calcium and Barium Hydroxide Nanoparticles for Wall
855 Painting Consolidation, Chem. – A Eur. J. 16 (2010) 9374–9382.
856 doi:10.1002/chem.201001443.
857 [22] C. Rodriguez-Navarro, E. Ruiz-Agudo, M. Ortega-Huertas, E. Hansen,
858 Nanostructure and Irreversible Colloidal Behavior of Ca(OH)2: Implications in
859 Cultural Heritage Conservation, Langmuir. 21 (2005) 10948–10957.
860 doi:10.1021/la051338f.
861 [23] M. Margalha, A. Silva, M. do Rosário Veiga, J. de Brito, R. Ball, G. Allen,
862 Microstructural Changes of Lime Putty during Aging, J. Mater. Civ. Eng. 25
863 (2013) 1524–1532. doi:doi:10.1061/(ASCE)MT.1943-5533.0000687.
864 [24] A. Moropoulou, A. Bakolas, P. Moundoulas, E. Aggelakopoulou, S.
865 Anagnostopoulou, Strength development and lime reaction in mortars for repairing
866 historic masonries, Cem. Concr. Compos. 27 (2005) 289–294.
867 doi:http://dx.doi.org/10.1016/j.cemconcomp.2004.02.017.
868 [25] S. Papatzani, K. Paine, J. Calabria-Holley, A comprehensive review of the models
869 on the nanostructure of calcium silicate hydrates, Constr. Build. Mater. 74 (2015)
870 219–234. doi:http://dx.doi.org/10.1016/j.conbuildmat.2014.10.029.
871 [26] V. Morales-Florez, N. Findling, F. Brunet, Changes on the nanostructure of
872 cementitius calcium silicate hydrates (C–S–H) induced by aqueous carbonation, J.
873 Mater. Sci. 47 (2012) 764–771. doi:10.1007/s10853-011-5852-6.
874 [27] R. Largent, Estimation de l' activite pouzzolanique, Bull. Liasons Lab. Pont
875 Chausees. 93 (1978) 61–65.
876 [28] J.A. Kostuch, V. Walters, T.R. Jones, High performance concretes incorporating
877 metakaolin: a review, in: R.K. Dhir, M.R. Jones (Eds.), Concr. 2000 Econ. Durable
878 Constr. Through Excell., E&FN SPON, London, 1996: pp. 1799–1811.

879 [29] V.S. Ramachandran, J.J. Beaudoin, Handbook of Analytical Techniques in
880 Concrete Science and Technology, Principles, Techniques, and Applications,
881 Noyes publications, New Jersey , 2001.
882 [30] Renishaw Plc, WiRE software, (2016). http://www.renishaw.com/en/raman-
883 software-analysis--25909 (accessed December 7, 2016).
884 [31] Bruker, EVA software, (2016). https://www.bruker.com/products/x-ray-
885 diffraction-and-elemental-analysis/x-ray-diffraction/xrd-software/eva/technical-
886 details.html (accessed December 7, 2017).
887 [32] S. Papatzani, K. Paine, Polycarboxylate / nanosilica modified quaternary cement
888 formulations - enhancements and limitations - in press, Adv. Cem. Res. (2017).
889 doi:https://doi.org/10.1680/jadcr.17.00111.
890 [33] E.T. Carlson, H.A. Berman, Some observations on the calcium aluminate
891 carbonate hydrates, J. Res. Natl. Bur. Stand. (1934). 64 (1960) 333–341.
892 [34] R. Snellings, A. Salze, K.L. Scrivener, Use of X-ray diffraction to quantify
893 amorphous supplementary cementitious materials in anhydrous and hydrated
894 blended cements, Cem. Concr. Res. 64 (2014) 89–98.
895 doi:http://dx.doi.org/10.1016/j.cemconres.2014.06.011.
896 [35] S. Papatzani, Nanotechnologically modified cements: Effects on hydration,
897 microstructure and physical properties, University of Bath, 2014.
898 [36] W. Xie, Z. Gao, K. Liu, W.-P. Pan, R. Vaia, D. Hunter, et al., Thermal
899 characterization of organically modified montmorillonite, Thermochim. Acta. 367–
900 368 (2001) 339–350. doi:http://dx.doi.org/10.1016/S0040-6031(00)00690-0.
901 [37] Q. Zhou, R.L. Frost, H. He, Y. Xi, Changes in the surfaces of adsorbed para-
902 nitrophenol on {HDTMA} organoclay—The {XRD} and {TG} study, J. Colloid
903 Interface Sci. 307 (2007) 50–55. doi:http://dx.doi.org/10.1016/j.jcis.2006.11.016.

[38] R.J. Ball, G.L.A. Pesce, C.R. Bowen, G.C. Allen, Characterisation of Lime/Metakaolin Paste Using Impedance Spectroscopy, Key Eng. Mater. 517 (2012) 487–494. doi:10.4028/www.scientific.net/KEM.517.487.

[39] G.L. Pesce, C.R. Bowen, J. Rocha, M. Sardo, G.C. Allen, P.J. Walker, et al., Monitoring hydration in lime-metakaolin composites using electrochemical impedance spectroscopy and nuclear magnetic resonance spectroscopy, Clay Miner. 49 (2014) 341–358. doi:10.1180/claymin.2014.049.3.01.

[40] L. Vieille, I. Rousselot, F. Leroux, J.-P. Besse, C. Taviot-Guého, Hydrocalumite and Its Polymer Derivatives. 1. Reversible Thermal Behavior of Friedel's Salt: A Direct Observation by Means of High-Temperature in Situ Powder X-ray Diffraction, Chem. Mater. 15 (2003) 4361–4368. doi:10.1021/cm031069j.

[41] S.J. Mills, A.G. Christy, J.-M. Génin, T. Kameda, F. Colombo, Nomenclature of the hydrotalcite supergroup: natural layered double hydroxides, Mineral. Mag. 76 (2012) 1289–1336.

[42] J. Bouzaid, R.L. Frost, Thermal decomposition of stichtite, J. Therm. Anal. Calorim. 89 (2007) 133–135. doi:10.1007/s10973-005-7272-9.

[43] A. V Borhade, A.G. Dholi, D.R. Tope, S.G. Wakchaure, Solvothermal synthesis and crystal structure of aluminogermanate halide sodalites using organic solvent, Indian J. Pure Appl. Phys. 50 (2012) 576–582.

[44] M. Földvári, Handbook of the thermogravimetric system of minerals and its use in geological practice, 2011. doi:10.1556/CEuGeol.56.2013.4.6.

[45] K. Byrappa, M.K. Devaraju, P. Madhusudan, A.S. Dayananda, B.V.S. Kumar, H.N. Girish, et al., Synthesis and characterization of calcium aluminum silicate hydroxide (CASH) mineral, J. Mater. Sci. 41 (2006) 1395–1398. doi:10.1007/s10853-006-7413-y.

929 [46] S. Goñi, A. Guerrero, M.P. Luxán, A. Macías, Activation of the fly ash pozzolanic
930 reaction by hydrothermal conditions, Cem. Concr. Res. 33 (2003) 1399–1405.
931 doi:http://dx.doi.org/10.1016/S0008-8846(03)00085-1.
932 [47] A. Gameiro, A. Santos Silva, P. Faria, J. Grilo, T. Branco, R. Veiga, et al.,
933 Physical and chemical assessment of lime–metakaolin mortars: Influence of
934 binder:aggregate ratio, Cem. Concr. Compos. 45 (2014) 264–271.
935 doi:http://dx.doi.org/10.1016/j.cemconcomp.2013.06.010.
936 [48] S. Goñi, A. Guerrero, Accelerated carbonation of Friedel's salt in calcium
937 aluminate cement paste, Cem. Concr. Res. 33 (2003) 21–26.
938 doi:http://dx.doi.org/10.1016/S0008-8846(02)00910-9.
939 [49] T. Székely, G. Várhegyi, F. Till, The determination and use of the second
940 derivative thermogravimetric function (DDTG) and the calculation of the kinetic
941 constants of some decomposition reaction types, J. Therm. Anal. 5 (1973) 227–
942 237. doi:10.1007/BF01950371.
943
944

# 7. Appendix – Decomposition mass loss calculations

## 8 days – experimental mass loss calculations

**The following can be noted with respect to the results presented in Table 5 [equation 1 – $M_{CH}$ calculation].**

For the mass loss observed within 400-500ºC for 50%LP+50%nC:

$M_{CH}^{nC1}$ = 13.97% – 9.48%x50% = 9.2% [9.48% corresponds to the mass loss of nC1 within 400-500ºC (Table 3)].

$M_{CH}^{nC2}$ = 18.63% – 20.14%x50% = 8.6% [20.14% corresponds to the mass loss of nC2 within 400-500ºC (Table 3)].

It is interesting to note that: 10.53 + 13.97 = 24.5% ~ 50% x 44.8 % = 22.4% [precisely 50% nC1 decomposition mass loss (Table 3)] and

7.35 + 18.63 = 25.98% ~ 50% x 46 % = 23% [precisely 50% nC2 decomposition mass loss (Table 3)]

$M_{CH}^{nC3}$ = 8.88% – 1.0%x50% = 8.4% [1.0% corresponds to the mass loss of nC3 within 400-500ºC (Table 4)].

For the mass loss observed within 400-500ºC for 20%LP+80%nC:

$M_{CH}^{nC1}$ = 12.72% – 9.48%x80% = 5.14%, therefore significant reduction in $Ca(OH)_2$ was achieved by **80% nC1**.

963 $M_{CH}^{nC2}$ = 16.11% – 20.14%x80% = 0.0%, therefore significant reduction in $Ca(OH)_2$ was

964 achieved by **80% nC2**.

965 $M_{CH}^{nC3}$ = 3.6% – 1.0%x80% = 2.8%, therefore significant reduction of $Ca(OH)_2$ was achieved

966 by **80% nC3**.

967 **Calculation of decomposition of calcium carbonate [equation 2 – $M_{CC}$ calculation]**

968 $M_{CC} = M_{loss}^{600\text{-}800} – M_{NMt}^{600\text{-}800}$ x (%NMt)

969 For 50% nC1: $M_{CC}$ = 5.93% – 0x50% = 5.9%

970 For 50% nC2: $M_{CC}$ = 4.19% – 0x50% = 4.2%

971 For 50% nC3: $M_{CC}$ = 11.73% – 4.4x50% = 9.5%

972 For 80% nC1: $M_{CC}$ = 11.3% – 0x80% = 11.3%

973 For 80% nC2: $M_{CC}$ = 4.64% – 0x80% = 6.46%

974 For 80% nC3: $M_{CC}$ = 9% – 4.4x80% = 5.5%

975 Table Ap-1: Elaboration of experimental results at day 8

| | Experimental values | | | | | |
|---|---|---|---|---|---|---|
| **Sample** | **$M_{CH}$ (%)** Eq1 | **$M_{CC}$ (%)** Eq2 | **$MM_{CH}$** Eq3 | **$MM_{CC}$** Eq4 | **$MMcarb_{CH}$** | **$MM_{totCH}$** Eq5 |
| **50%LP+50%nC1** | 9.20 | 5.93 | 37.86 | 13.48 | 9.99 | 47.85 |
| **50%LP+50%nC2** | 8.60 | 4.19 | 35.39 | 9.52 | 7.05 | 42.44 |
| **50%LP+50%nC3** | 8.40 | 9.50 | 34.57 | 21.59 | 15.99 | 50.56 |
| **20%LP+80%nC1** | 5.15 | 11.30 | 21.15 | 25.68 | 19.02 | 40.17 |

| | | | | | | |
|---|---|---|---|---|---|---|
| **20%LP+80%nC2** | 0.00 | 6.46 | 0.00 | 14.77 | 10.94 | 10.94 |
| **20%LP+80%nC3** | 2.80 | 5.50 | 11.52 | 12.50 | 9.26 | 20.78 |

## 8 days – theoretical mass loss calculations

Estimation of theoretical mass loss attributed to CH:

Furthermore, theoretically, if nC1/2/3 and LP were not engaged in reactions, disregarding carbonation, according to the mass losses recorded in Table 2 to 5 **between 400-500°C** for:

50% LP+50% nC1 the mass loss should have been 50%x20.20 + 50%x9.48 = 14.8% > 13.97

50% LP+50% nC2 the mass loss should be 50%x20.20 + 50%x20.14 = 20.2% > 18.63

50% LP+50% nC3 the mass loss should be 50%x20.20 +50%x(1)= 10.6% > 8.88

20% LP+80% nC1 the mass loss should be 20%x20.20 + 80%x9.48 = 11.6% < 12.72

20% LP+80% nC2 the mass loss should be 20%x20.20 + 80%x20.14 = 20.0% > 16.11

20% LP+80% nC3 the mass loss should be 20%x20.20 + 80%x1 = 4.8% > 3.6

Estimation of theoretical mass loss attributed to the **decomposition of calcium carbonate [equation 2 – $M_{CC}$ calculation]:**

$M_{CC} = M_{loss}^{600\text{-}800} - M_{NMt}^{600\text{-}800}$ x (%NMt)

For 50% nC3: $M_{CC}$ =3.52x50% + 4.4x50% = 4%

For 80% nC3: $M_{CC}$ = 3.52x20% + 4.4x80% = 4.2%

994 Table Ap-2: Elaboration of theoretical values at day 8

| | Theoretical values | | | | | |
|---|---|---|---|---|---|---|
| **Sample** | **$M_{CH}$ (%)** Eq1 | **$M_{CC}$ (%)** Eq2 | **$MM_{CH}$** Eq3 | **$MM_{CC}$** Eq4 | **$MMcarb_{CH}$** | **$MM_{totCH}$** Eq5 |
| **50%LP+50%nC1** | 14.80 | 0.00 | 60.91 | 0.00 | 0.00 | 60.91 |
| **50%LP+50%nC2** | 20.20 | 0.00 | 83.13 | 0.00 | 0.00 | 83.13 |
| **50%LP+50%nC3** | 10.60 | 4.00 | 43.62 | 9.10 | 6.70 | 50.32 |
| **20%LP+80%nC1** | 11.60 | 0.00 | 47.74 | 0.00 | 0.00 | 47.74 |
| **20%LP+80%nC2** | 20.00 | 0.00 | 82.30 | 0.00 | 0.00 | 82.30 |
| **20%LP+80%nC3** | 4.80 | 4.20 | 19.75 | 9.50 | 7.00 | 26.75 |

995

996 ## 8 months – experimental mass loss calculations

997 **The following can be noted with respect to the results presented in Table 7 [equations 1**
998 **and 2].**

999 1: At 100% LP, the mass loss related to $Ca(OH)_2$ was 21.24%, therefore for 50% LP it would be
1000 10.6% and for 20% LP, the mass loss would be 4.2%.

1001 2: for the mass loss observed within 400-500ºC: 12.47% – 9.48%x50% = 7.73% < 10.6%,
1002 hence some reduction of $Ca(OH)_2$ was achieved by 50% nC1.

1003 3: for the mass loss observed within 400-500ºC: 17.26% – 20.14%x50% = 7.19% < 10.6%,
1004 therefore significant reduction of $Ca(OH)_2$ was achieved by 50% nC2.

1005 Moreover, it is interesting to add the two underlined mass losses:

2A: 10.93 + 12.47 = 23.4% ~ 50% x 44.8 % = 22.4% (50% nC1 decomposition mass loss), therefore, yielding absolute accuracy.

3A: 6.9 + 17.26 = 24.16% ~ 50% x 46.09 % = 23.5% (50% nC2 decomposition mass loss), therefore, yielding absolute accuracy.

4: For the mass loss observed within 400-500°C: 9.23% – 1.0%x50% = 8.73% < 10.6%, therefore significant reduction of $Ca(OH)_2$ was achieved by 50% nC3.

5: For the mass loss observed within 400-500°C: 8.1% – 9.48%x80% = 0.52% <4.2%, therefore almost elimination of $Ca(OH)_2$ was achieved by 80% nC1.

6: For the mass loss observed within 400-500°C: 11.37% – 20.14%x80% = 0%< 4.2%, therefore elimination of $Ca(OH)_2$ was achieved by 80% nC2.

7: For the mass loss observed within 400-500°C: 1.42% – 1.0%x80% = 0.62% < 4.2%, therefore almost elimination of $Ca(OH)_2$ was achieved by 80% nC3.

**Calculation of decomposition of calcium carbonate [equation 2]**

$M_{CC} = M_{loss}^{600\text{-}800} – M_{NMt}^{600\text{-}800}$ x (%NMt)

For 50% nC1: $M_{CC}$ = 5.57% – 0x50% = 5.6%

For 50% nC2: $M_{CC}$ = 3.4% – 0x50% = 3.4%

For 50% nC3: $M_{CC}$ = 2.94% – 4.4x50% = 0.7%

For 80% nC1: $M_{CC}$ = 5.5% – 0x80% = 5.5%

For 80% nC2: $M_{CC}$ = 4.93% – 0x80% = 4.9%

For 80% nC3: $M_{CC}$ = 3% – 4.4x80% = 0.0%

Table Ap-3: Elaboration of experimental values at month 8

| Experimental values | | | | | | |
|---|---|---|---|---|---|---|
| **Sample** | **$M_{CH}$** | **$M_{CC}$** | **$MM_{CH}$** | **$MM_{CC}$** | **$MM_{carbCH}$** | $MM_{totCH}$ |
| | Eq1 | Eq2 | Eq3 | Eq4 | | Eq5 |
| **50%LP+50%nC1** | 7.73 | 5.57 | 31.81 | 12.66 | 9.37 | 41.18 |
| **50%LP+50%nC2** | 7.19 | 3.40 | 29.59 | 7.73 | 5.72 | 35.31 |
| **50%LP+50%nC3** | 8.73 | 0.73 | 35.93 | 1.66 | 1.23 | 37.16 |
| **20%LP+80%nC1** | 0.52 | 5.50 | 2.14 | 12.50 | 9.25 | 11.39 |
| **20%LP+80%nC2** | 0.00 | 4.93 | 0.00 | 11.20 | 8.29 | 8.29 |
| **20%LP+80%nC3** | 0.62 | 0.00 | 2.55 | 0.00 | 0.00 | 2.55 |

## 8 months – theoretical mass loss calculations

Disregarding carbonation, theoretically, according to the mass losses recorded in Table 2 to 4 and Table **7** between **400-500°C** for:

50% LP+50% nC1 the mass loss should be 50%x(21.24) + 50%x9.48 = 15.4% > 12.47

50% LP+50% nC2 the mass loss should be 50%x21.24 + 50%x20.14 = 20.7% > 17.26

50% LP+50% nC3 the mass loss should be 50%x21.24 + 50%x1 = 11.1% > 9.23

20% LP+80% nC1 the mass loss should be 20%x21.24 + 80%x9.48 = 11.8% > 8.10

20% LP+80% nC2 the mass loss should be 20%x21.24 + 80%x20.14 = 20.4% > 11.37

20% LP+80% nC3 the mass loss should be 20%x21.24 + 80%x1= 5.0% > 1.4

Estimation of theoretical mass loss attributed to the **decomposition of calcium carbonate [equation 2 – $M_{CC}$ calculation]:**

$M_{CC} = M_{loss}^{600\text{-}800} - M_{NMt}^{600\text{-}800}$ x (%NMt)

For 50% nC3: $M_{CC}$ =3.52x50% + 4.4x50% = 4%

For 80% nC3: $M_{CC}$ = 3.52x20% + 4.4x80% = 4.2%

Table Ap-4: Elaboration of theoretical values at month 8

| | Theoretical values | | | | | |
|---|---|---|---|---|---|---|
| **Sample** | **$M_{CH}$ (%)** Eq1 | **$M_{CC}$ (%)** Eq2 | **$MM_{CH}$** Eq3 | **$MM_{CC}$** Eq4 | **$MMcarb_{CH}$** | **$MM_{totCH}$** Eq5 |
| **50%LP+50%nC1** | 15.40 | 0.00 | 63.37 | 0.00 | 0.00 | 63.37 |
| **50%LP+50%nC2** | 20.70 | 0.00 | 85.19 | 0.00 | 0.00 | 85.19 |
| **50%LP+50%nC3** | 11.10 | 4.00 | 45.68 | 9.10 | 6.70 | 52.41 |
| **20%LP+80%nC1** | 11.80 | 0.00 | 48.56 | 0.00 | 0.00 | 48.56 |
| **20%LP+80%nC2** | 20.40 | 0.00 | 83.95 | 0.00 | 0.00 | 83.25 |
| **20%LP+80%nC3** | 5.00 | 4.20 | 20.58 | 9.50 | 7.00 | 27.65 |